KEM01
SAFE OPERATIONAL BANDWIDTH OF GAS STORAGE RESERVOIRS

Project Review (Dec.2017 – Jan.2019)

Pietro Teatini, Claudia Zoccarato, Massimiliano Ferronato, Andrea Franceschini, Matteo Frigo, Giovanni Isotton, Carlo Janna

Dept. ICEA - University of Padova

June 24th, 2021

Outline

- **Project aims**
- **Project structure**
- **Literature review (WP1)**
  - in The Netherlands
  - in Italy
- **Model set-up (WP2)**
- **Sensitivity & Scenarios (WP3-WP5-WP6)**
- **Outcome analysis (WP4-WP7)**
  - comparing
  - ranking
  - guidelines for safe operational bandwidths
- **Ongoing and planned research on the topic addressed by KEM01**

Project Aims

INVESTIGATE:

- the geomechanical hazards and risks associated with gas storage in Underground Gas Storage (UGS) reservoirs
- how possible drivers of fault reactivation can combine in UGS to increase the hazard of (significant) seismic events and/or even induced "un-expected" (micro-) seismicity

"EXPECTED" INDUCED SEISMICITY

- primary production (PP) with large pressure drop
- fluid injection (CO_2 sequestration, waste water disposal, fracking) with significant pressure increase

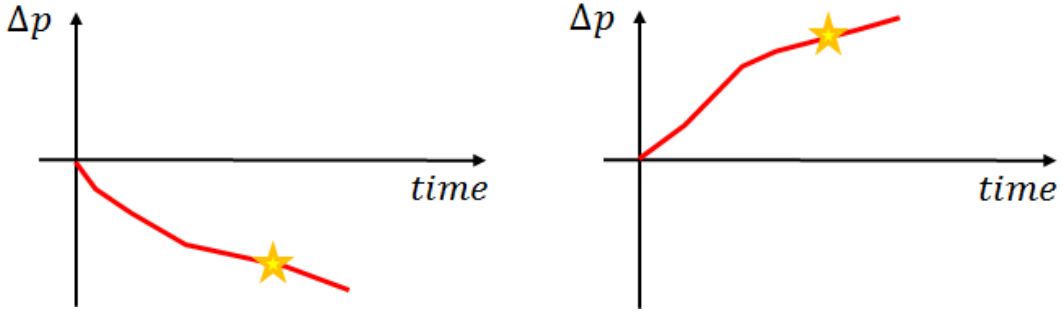

"UN-EXPECTED" INDUCED SEISMICITY

- when the pressure is within a range already experienced (UGS with $p<p_{initial}$)

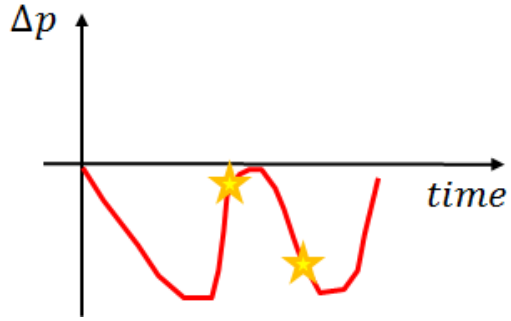

Project Structure

PHASE 1:

- **WP1** – Bibliographic review: inventory of possible mechanisms of fault reactivation induced by fluid injection/production in UGS
- **WP2** – Conceptual model and definition of the potential driving mechanisms (simplified representative geological setting of Dutch UGS)
- **WP3** – Modelling scenarios and mechanisms of fault reactivation proposed in WP2 investigated using M3E_GEPS3D
- **WP4** – Analysis of modelling results: (i) ranking the simulated scenarios (ii) weighting the critical factors

PHASE 2 (Phase 1 follow-up):

- **WP5** – Testing the proposed updates. The effect of the various modifications has been tested and the updated "reference" scenario has been defined
- **WP6** – Modelling scenarios. The scenarios investigated in WP3 have been re-evaluated taking into account the pressure change within the faults and the updated features of the salt caprock. A few more combined mechanisms have been investigated
- **WP7** – Final report. Based on the previous outcomes, in particular the numerical results provided in WP3, WP5 and WP6, the report aims at providing a few general rules to define a "safe operational bandwidth of gas storage reservoirs"

WP1 – Bibliographic review

RESERVOIR	LOCATION	TYPE	STAGE	ACTIVATED FAULT GEOMETRY	DEPTH			MAGNITUDE		
					below	reservoir	above	≤1	1 - 3	≥3
Norg	The Netherlands	UGS	PP; UGS	Slip motion on a sub-vertical NW-SE fault (PP) and a sub-vertical compressive SW-NE fault (UGS)		x			x (2)	
Grijpskerk	The Netherlands	UGS	UGS	large uncertainty to locate active faults					x (2)	
Bergermeer	The Netherlands	UGS	PP;CG;UGS	strike: SSW; dip: 60-65		x		x (1 - CG)		x (4 - PP)
Duvernay Formation	Canada	HF	PT	strike-slip motion on subvertical, ~-S/E-W oriented faults	x	x			x	x (4.1)
Castor	Spain	UGS	PT	secondary fault was activated during the 2013 earthquake sequence instead of the Amposta fault	x	x			x	x (4.3)

Inventory of induced seismicity cases according to reservoir development stage, event focal mechanism and magnitude, and hypocenter location with respect to the developed formation and the fault geometry. PP=primary production; UGS=underground gas storage; CG=cushion gas; PT=post-treatment; HF=hydraulic fracturing

WP1 – Bibliographic review

RESERVOIR	LOCATION	TYPE	STRESS REGIME	SEISMIC NETWORK	RESERVOIR INFO		
					depth	thickness	production history
Norg	The Netherlands	UGS		micro-seismic network in deep wells	2670	140	primary production started in 1983 until 1995 with a max DP of about 117 bar; UGS started in 1995-1997 with a DP for cycle of about 57 bar
Grijpskerk	The Netherlands	UGS			3300	220	primary production started in 1993 until 1994 with a max DP of about 53 bar; UGS started in 1997 with a DP for cycle of about 127 bar
Bergermeer	The Netherlands	UGS	sigma_v = 25 Mpa; sigma_h_min = 9 Mpa (effective stress); initial direction of the minimum horizontal stress is oriented NE-SW	down-hole micro-seismic network	2200	200	primary production started in 1971 until 2006 with a max DP of about 213 bar; no activity between 2007 and 2010; cushion gas injection between 2010 and 2012; UGS started in 2013
Duvernay Formation	Canada	HF	strike-slip regime, oriented at ~45°	regional & local networks	2600-4000	25-60	average mean injection pressure = 62.5 Mpa
Castor	Spain	UGS	graben structure with two families of active faults; the maximum horizontal stress equal to the vertical stress and points to the NE; the minimum horizontal stress equal to 0.7 × vertical stress	Spanish National Network	1800-2000	150-200	initial reservoir pressure = 190 bar; max Dp during primary production = 5 bar. During the injection period the maximum pressure increase observed in the Castor field was 7.6 bar above the initial formation pressure

Inventory of induced seismicity: stress regime and reservoir info

NORG

- four blocks separated by minor non-sealing faults
- the virgin average pressure in Block no. 2 was 327 bar, with a minimum value around 190 bar recorded in 1995
- the first seismic event occurred in 1993 during the primary production, while the second one was recorded in 1999 soon after the beginning of the UGS operations
- gradient for the vertical stress is estimated at 2.16 bar/10 m, the minimum / maximum horizontal stress at 1.63 bar/10 m and 1.92 bar/10 m

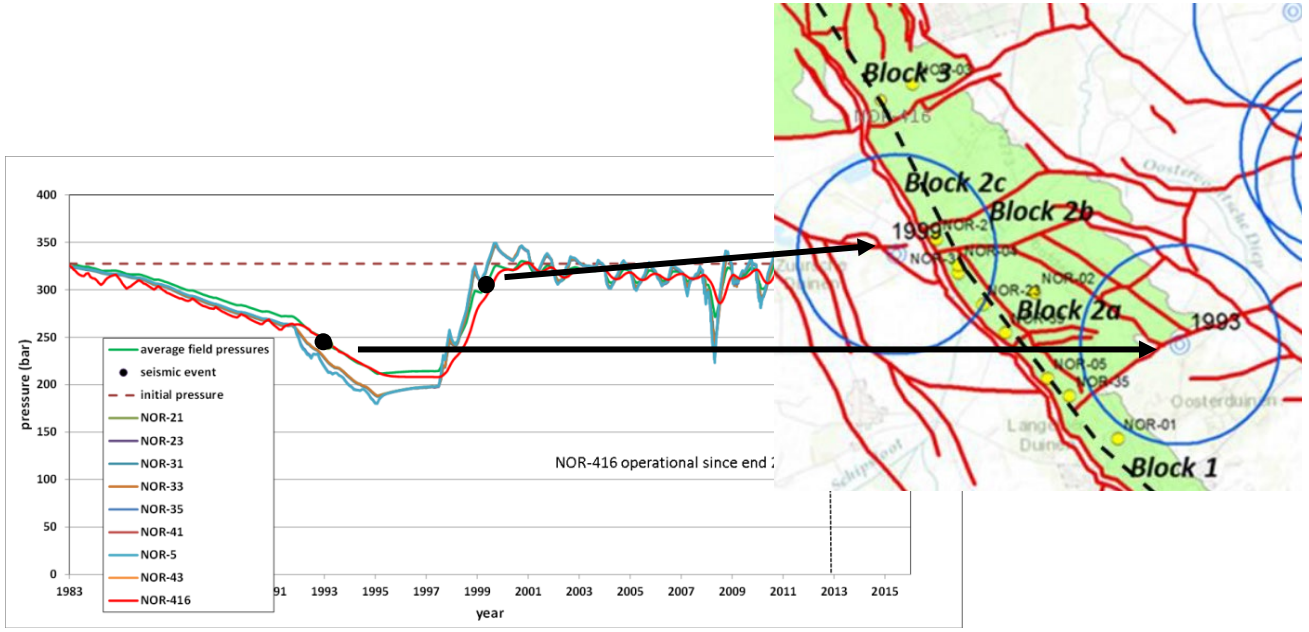

Pressure evolution in time at the Norg UGS field. The location of the two seismic events in 1993 and 199 are reported

GRIJPSKERK

- two seismic events have been detected, the first in 1997 (M=1.3) and the second in 2015 (M=1.5)
- both events occurred during the production phase at an average pressure of about 280 bar and at a flow rate of 9 million m^3/day
- large uncertainties associated with the hypocenter location

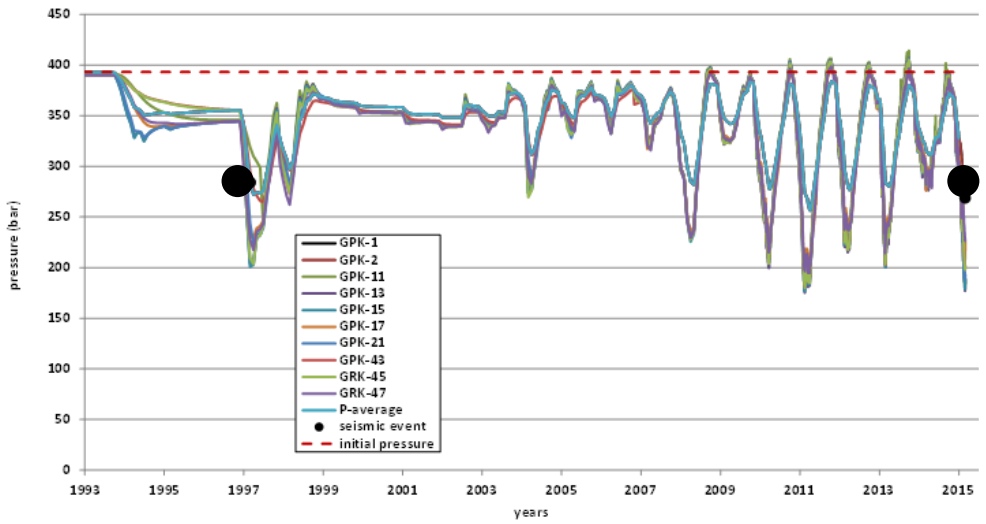

Pressure evolution in time at the Grijpskerk UGS field. The location of the two seismic events in 1997 and 2015 are reported

BERGERMEER

- the gas field consists of two reservoir blocks, which are intersected by a partially sealing Central fault
- 4 seismic events have been detected in 1994 and 2001 during primary production phase. The events are of magnitude in the range 3.0-3.5 and located at the tip of the central fault
- during injection of cushion gas some small seismic events were detected with a largest magnitude of M=0.7 recorded in 2013
- during annual cycles of gas injection and production, the Central fault is not critically stressed and the predicted stress changes lie in the elastic region. The fault slip is deemed to be unlikely

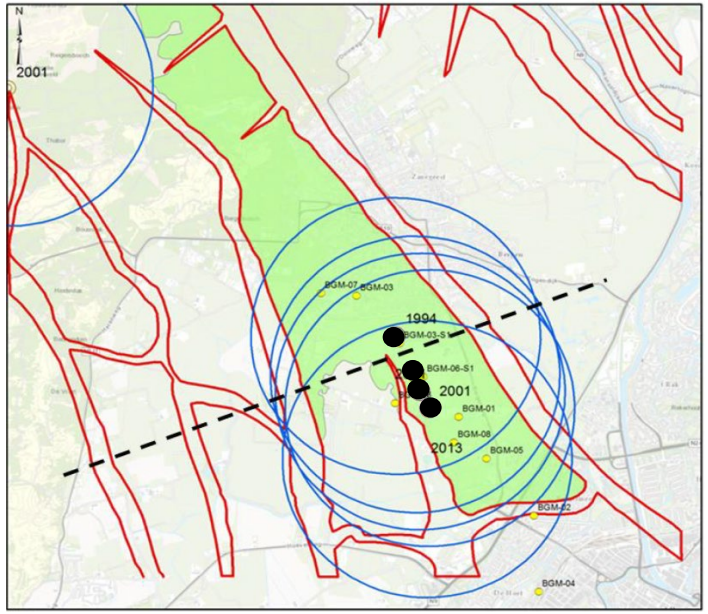

Map of the Bergermeer UGS field. The location of the seismic events from 1994 and 2013 are reported

WP1 – A UGS case study in Italy

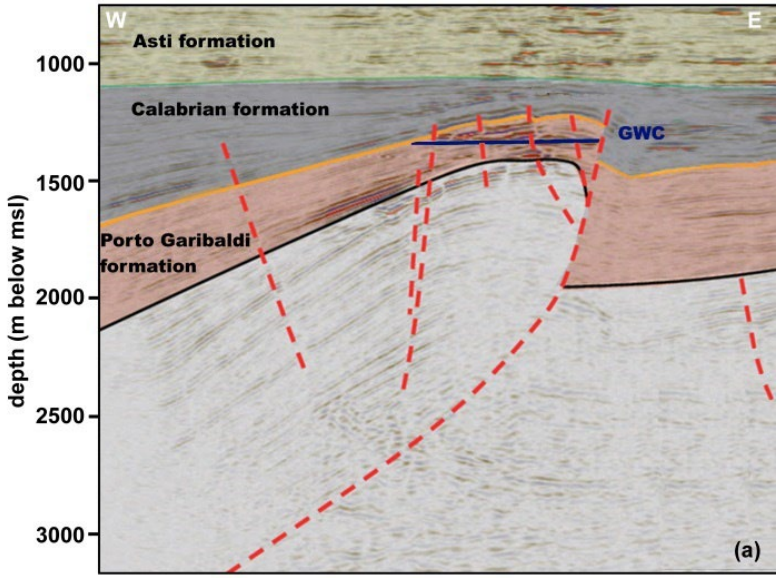

Seismic section

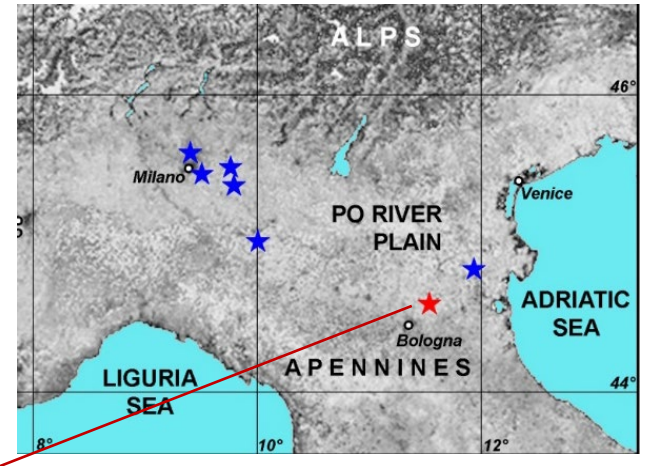

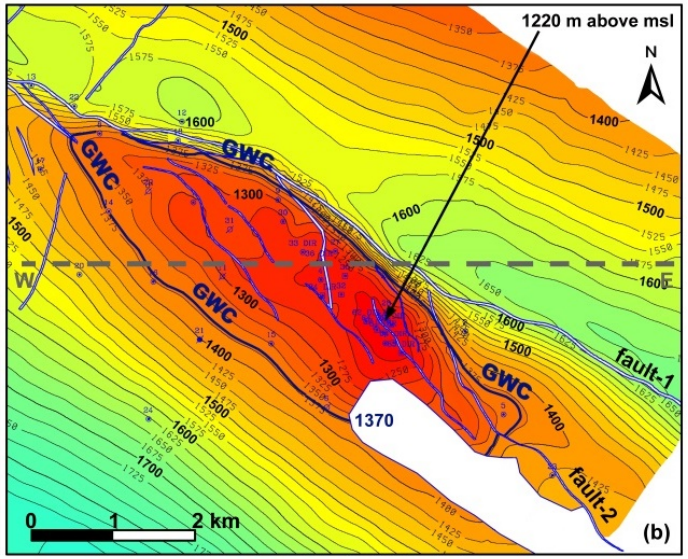

Depth of the reservoir top

Can UGS activities be responsible for the recorded seismicity?

Micro-seismicity recorded by the local micro-seismic borehole network in the area surrounding the Emilia field from 1979 to July 2013

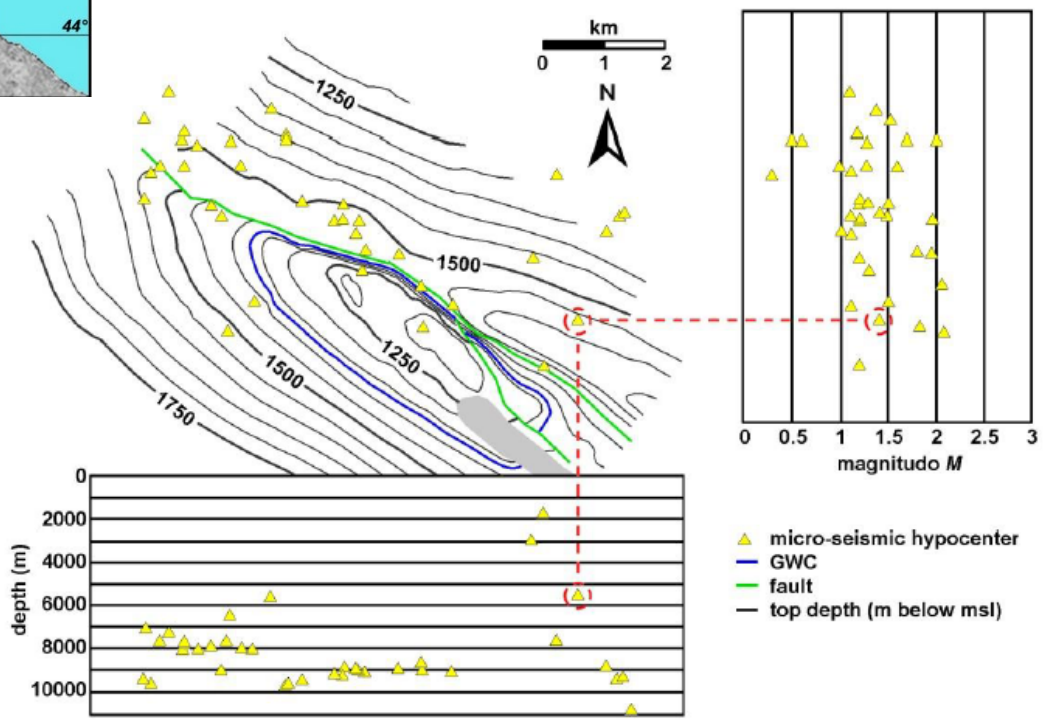

WP1 – A UGS case study in Italy

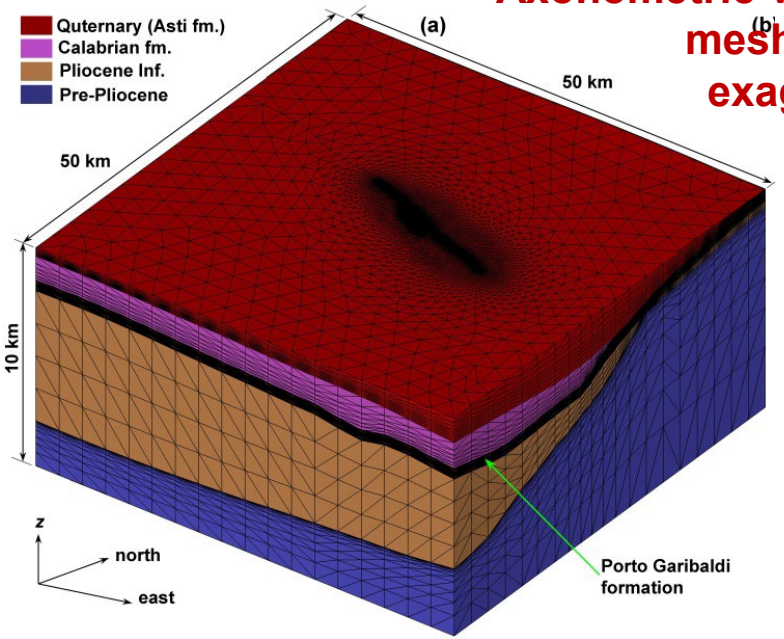

Axonometric view of the 3D mesh. The vertical exaggeration is 5

354'611 nodes
2'154'316 FEs
26'274 IEs

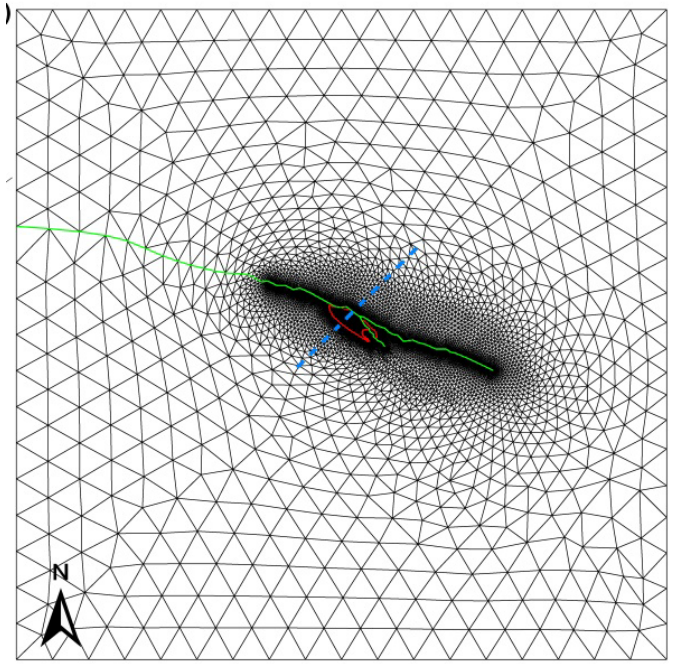

Grid plane view. The trace of the field (in red) and the faults (in green) confining northward and crossing the reservoir and the waterdrive are highlighted

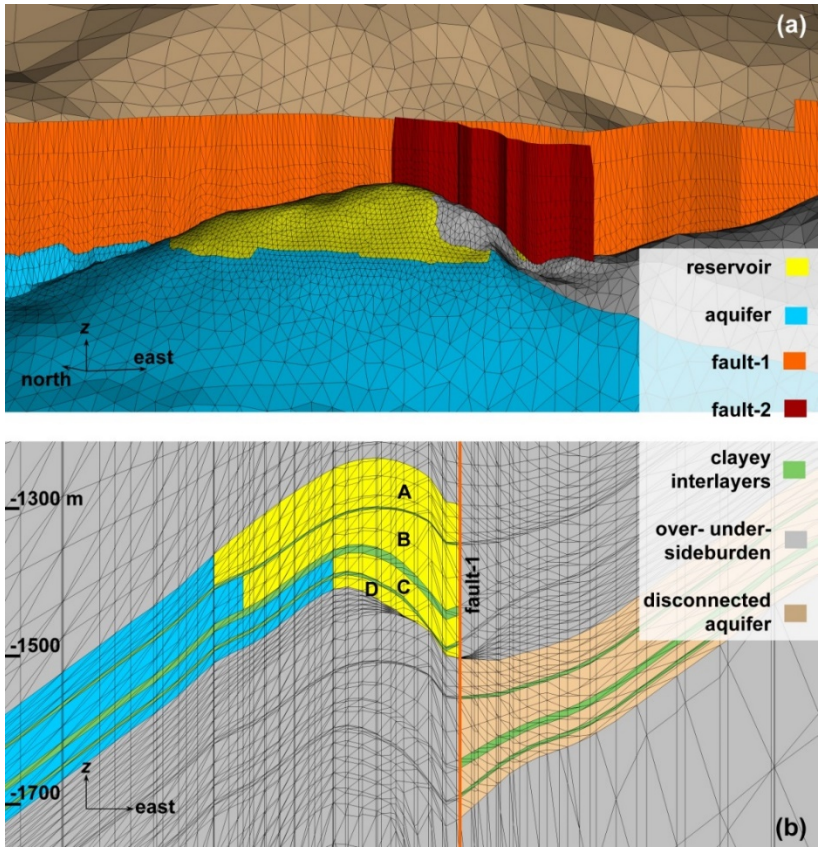

(a) Axonometric detail and (b) vertical southwest-northeast cross-section of the 3D FE-IE model of the Emilia gas field showing different portions of the geologic system.

WP1 – A UGS case study in Italy

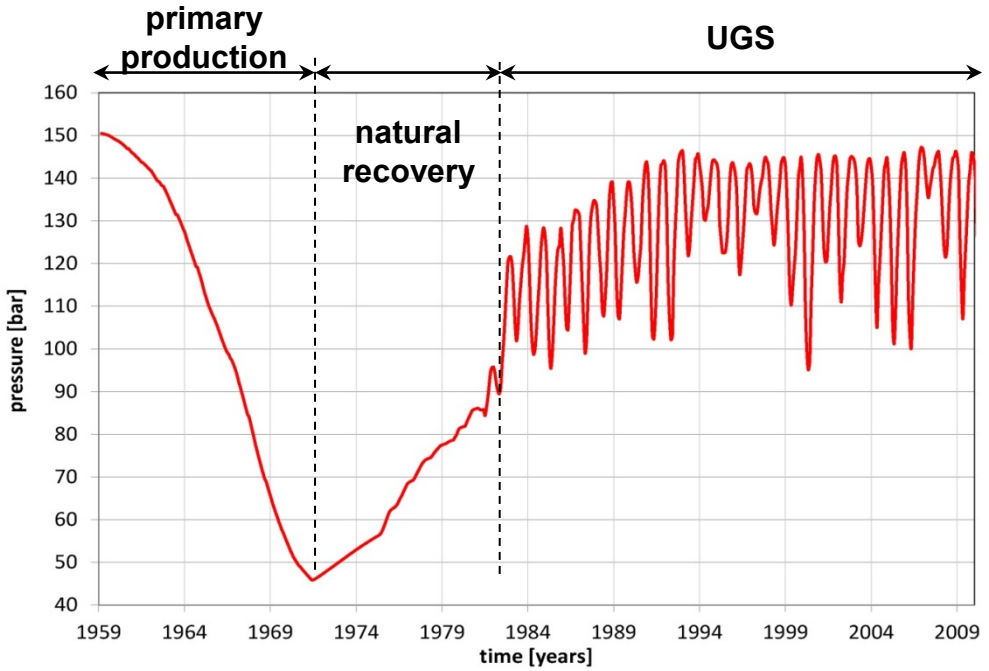

Average pore pressure behavior in the A layer

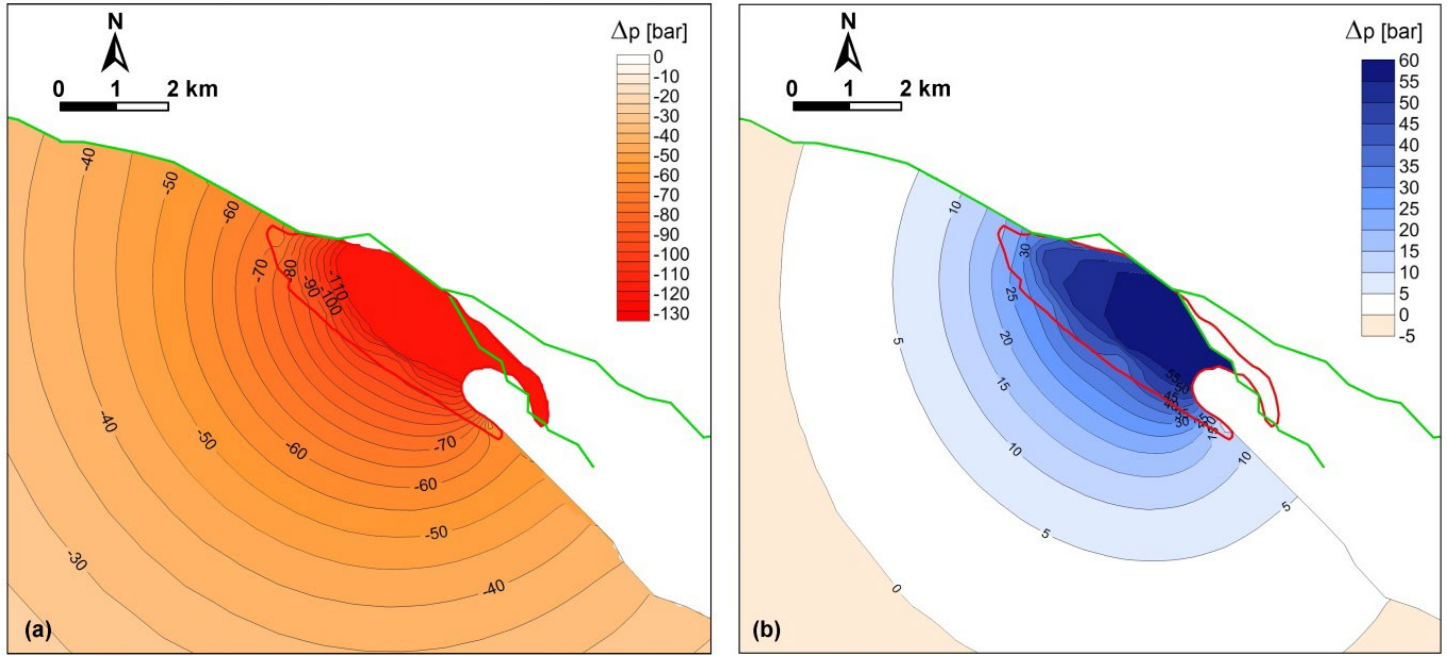

(a) Pore pressure decline (bars) in level A at the end of the field production life (1971) and (b) pore pressure increase during a UGS injection cycle from April to November 2006

WP1 – A UGS case study in Italy

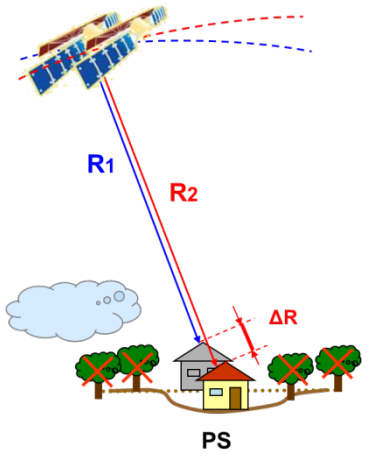

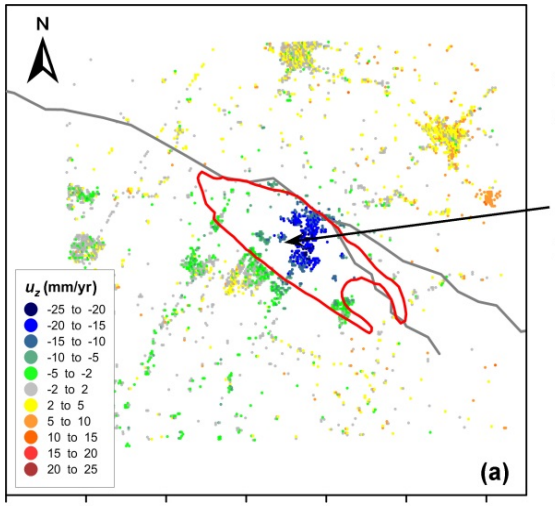

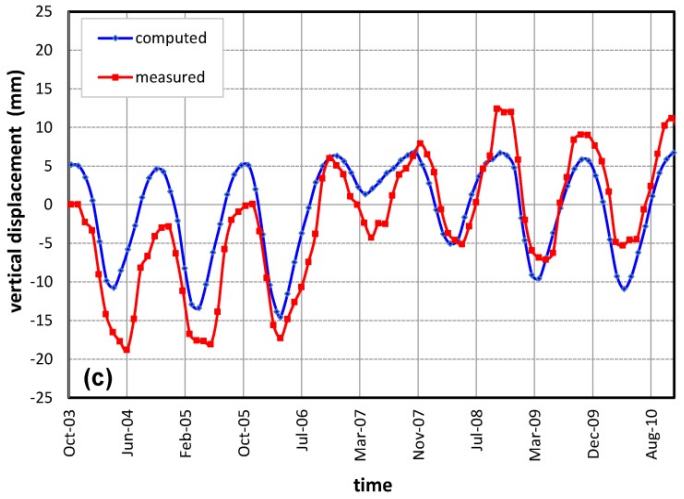

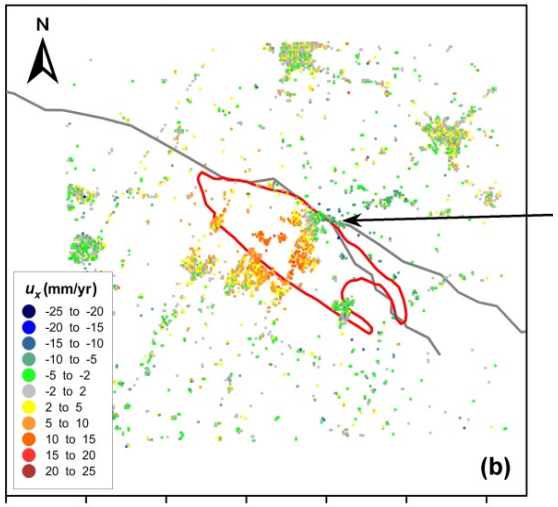

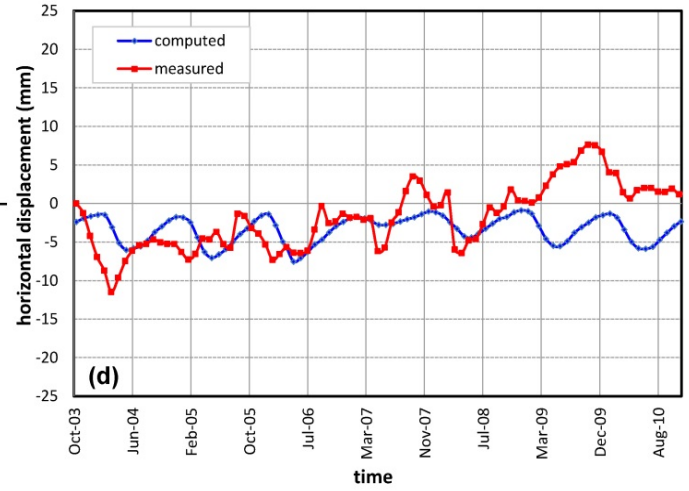

(a) Vertical and (b) west-east horizontal displacements (mm) as measured by PSInSAR above the Emilia field from 11/2004 to 04/2005. Match of the simulated (c) vertical and (d) horizontal movement with the satellite displacement

Basin-scale constitutive relationship (anisotropy):

$$c_M = 0.01241\ \sigma_z^{-1.1342}$$

from RMT (virgin loading condition)

$$\sigma_z^* = 0.12218\,|z|^{1.0766}$$

from density logs

β	ν_h	ν_z	γ	s
3.0	0.15	0.25	1.0	5.0

$\beta = E_h / E_z$ $\quad \gamma = G_h / G_z$ $\quad s = c_{M,I} / c_{M,II}$

from calibration (PSInSAR)

WP1 – A UGS case study in Italy

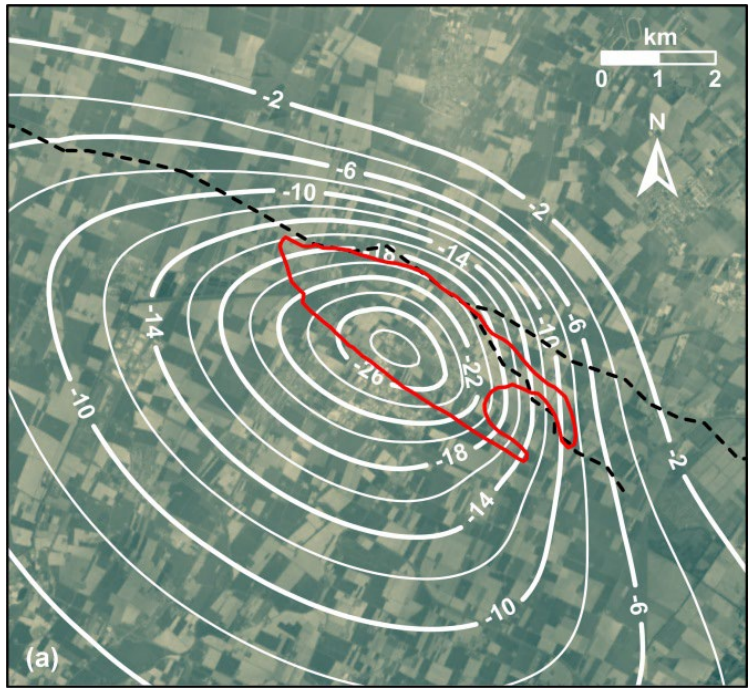

Land subsidence (cm) at the end the Emilia field production life (1971) as predicted by the FE-IE model

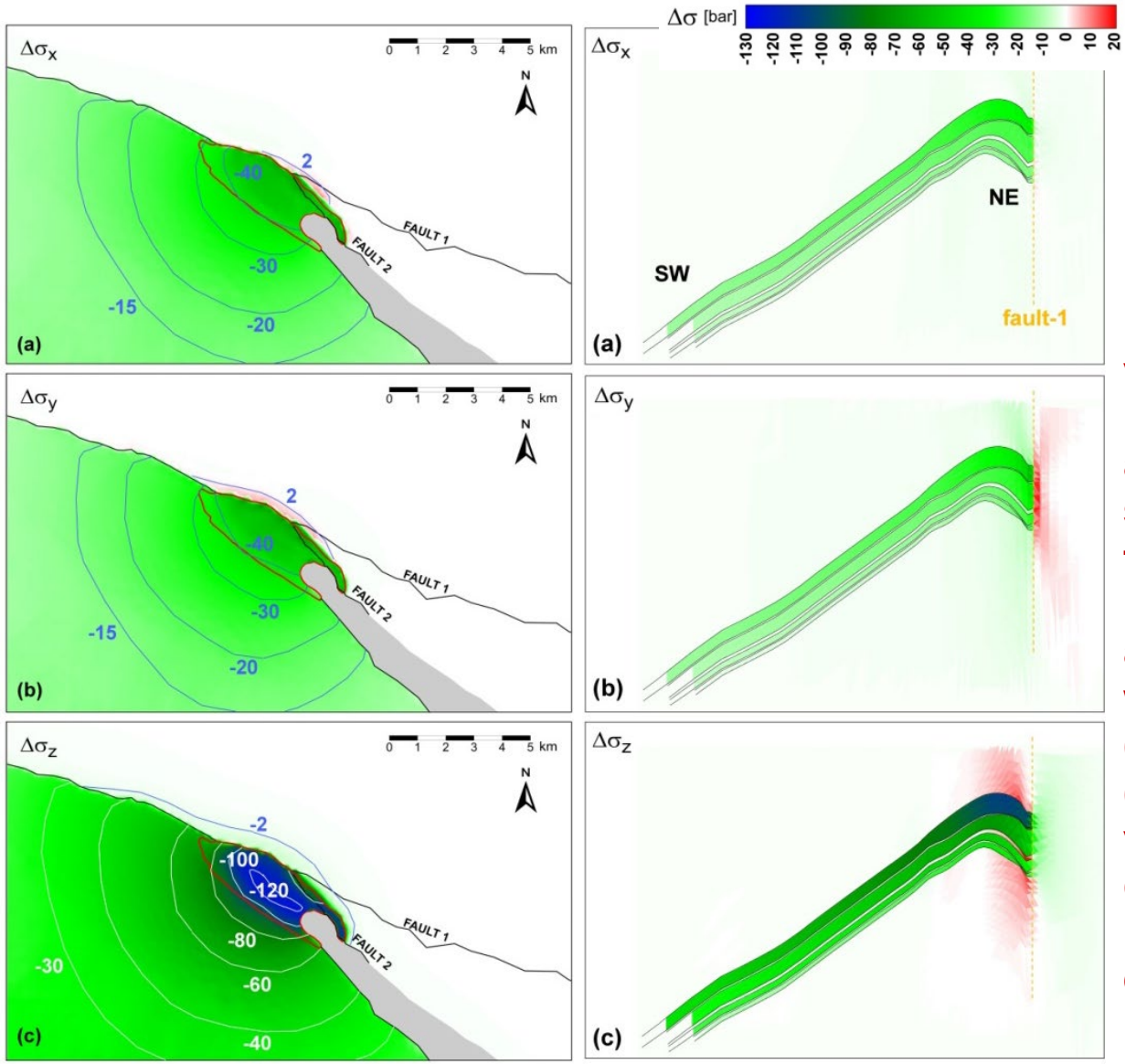

Normal stress variations (bar) in level A and in a vertical cross-section through the top of the Emilia gas field along (a) the west-east ($\Delta\sigma_x$), (b) north-south ($\Delta\sigma_y$), and (c) vertical ($\Delta\sigma_z$) directions in 1971, i.e. at the end of the field production life

WP1 – A UGS case study in Italy

Scenario A

- cohesion *c* =10 bar on the fault surface;
- friction angle = 30°;
- initial stress regime: compressive regime $\sigma_{h1} = \sigma_v \nu_h / (1- \nu_z)) = 0.3\ \sigma_v$
  $\sigma_{h2} = (\sigma_v + \sigma_{h1})/2 = 0.65\ \sigma_v$

Scenario B

- *c* = 0 bar;
- friction angle = 30°;
- initial stress regime: normal regime, $\sigma_{h1} = \sigma_{h2} = \sigma_v \nu_h / (1- \nu_z) = 0.3\ \sigma_v$

Scenario C

- *c* = 0 bar;
- friction angle = 30°;
- initial stress regime: compressive regime

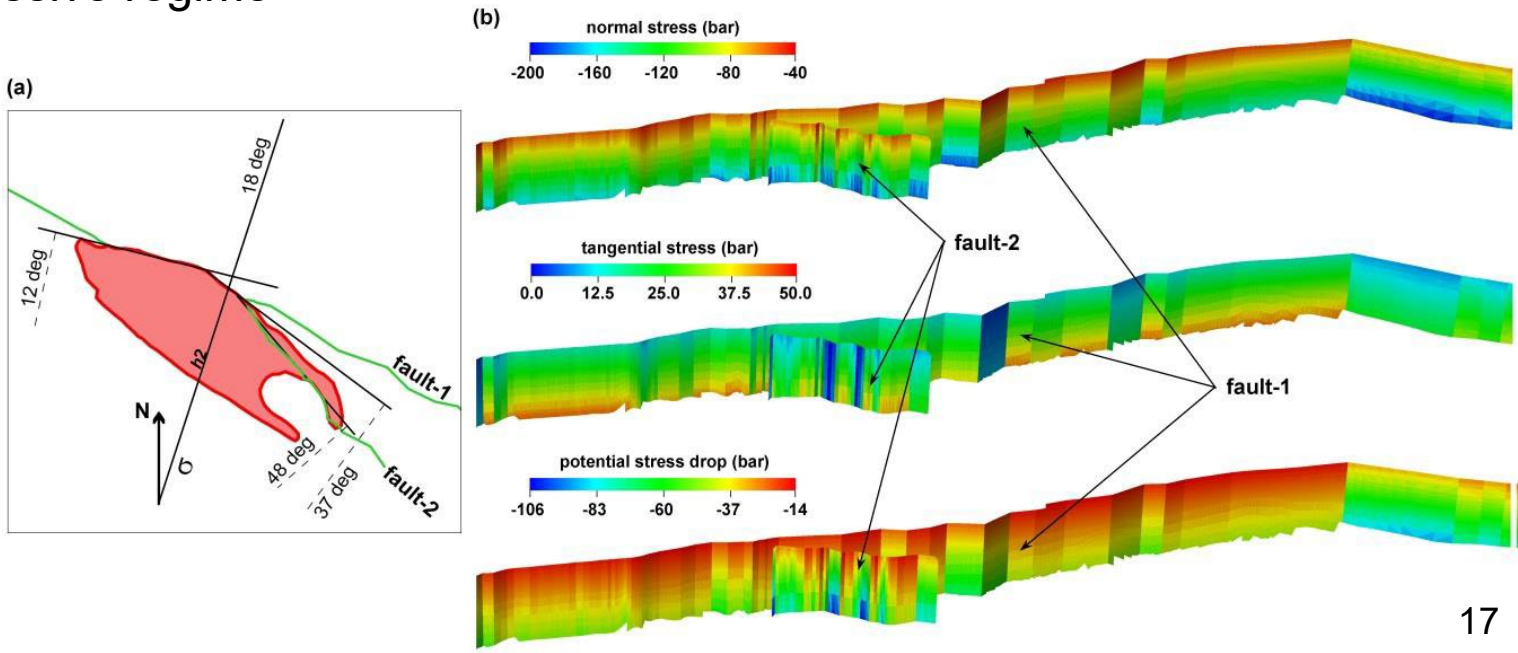

(a) Direction of the maximum horizontal stress in the horizontal plane σ_{h2}. (b) Initial normal and tangential stress and potential stress drop on the faults with scenario A

WP1 – A UGS case study in Italy

Perspective view on the fault discretization with the cumulative slip between 1959 and 1971, i.e. during the primary production life of the Emilia reservoir, as computed by the IE solution in (a) scenario A and (b) scenario (B). Vertical exaggeration is 5.

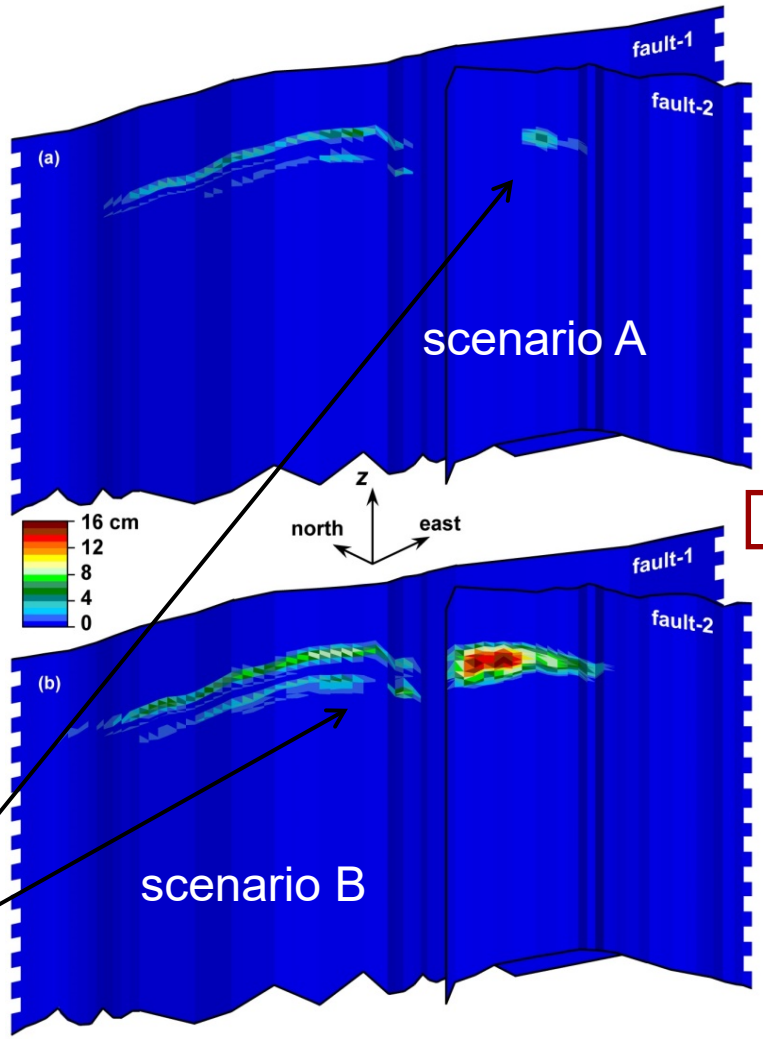

activation at the reservoir depth only

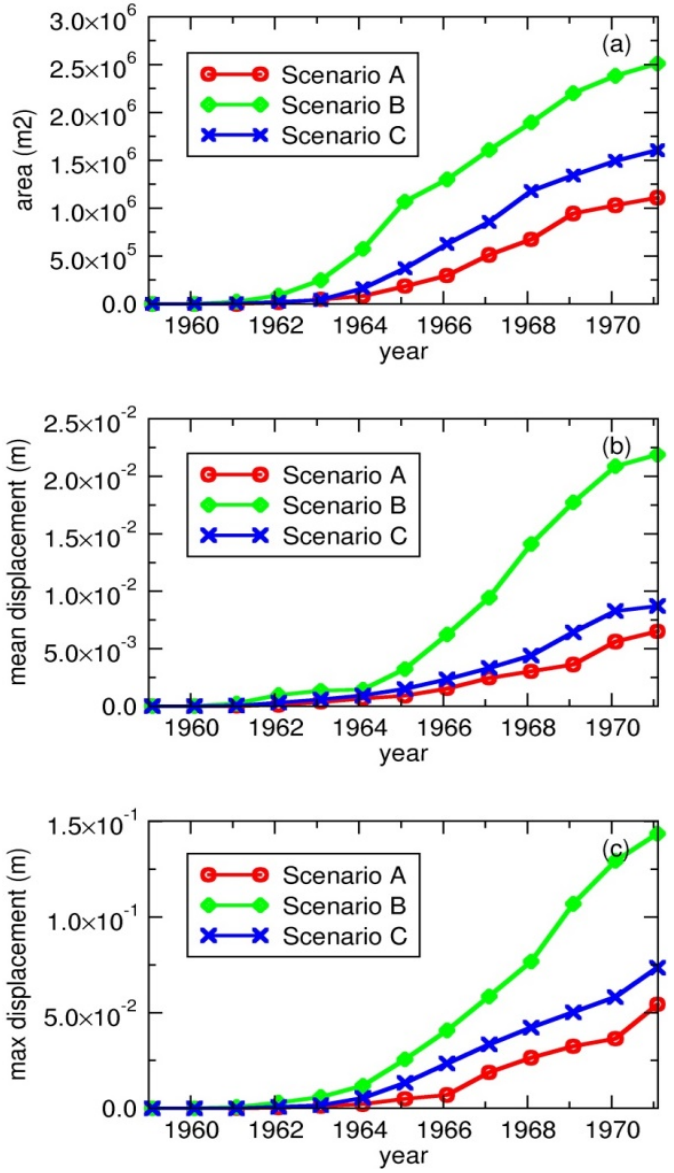

Area A, and average (s_a) and maximal (s_{max}) yearly slip of the activated portion of the faults during the primary development of the Emilia reservoir for the three scenarios addressed by the study

WP2 - Model set-up

Norg: sketch of the main faults

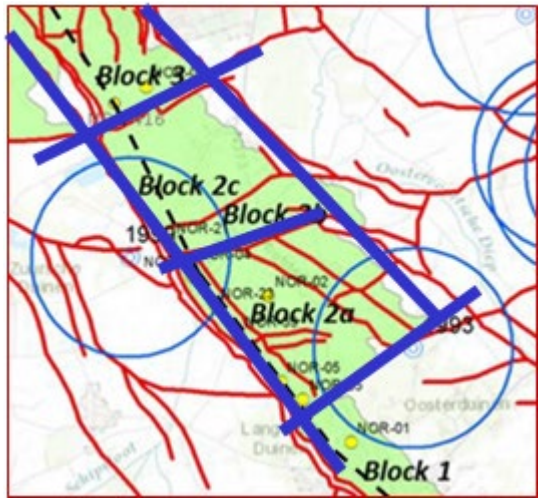

Bergermeer: sketch of the main faults

Representative geometrical configuration

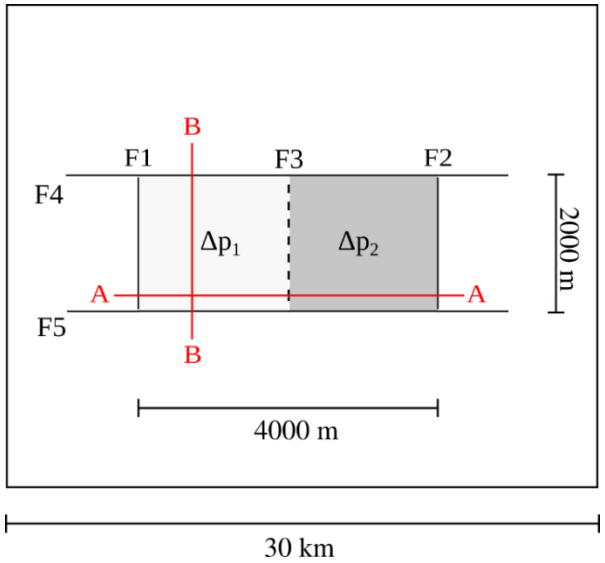

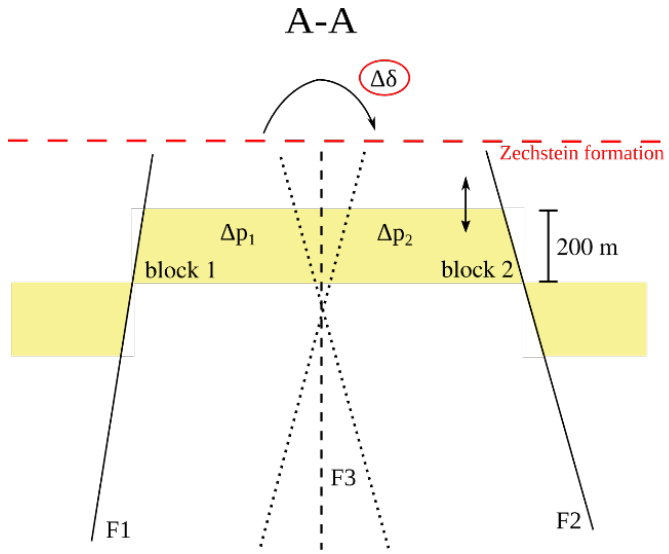

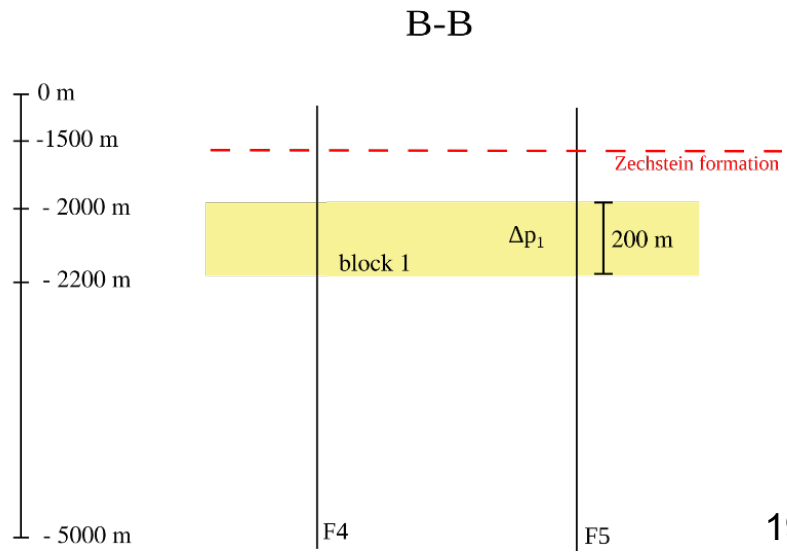

WP2 - Modelling Approach

Perspective view of possible IE elements in a 3D setting

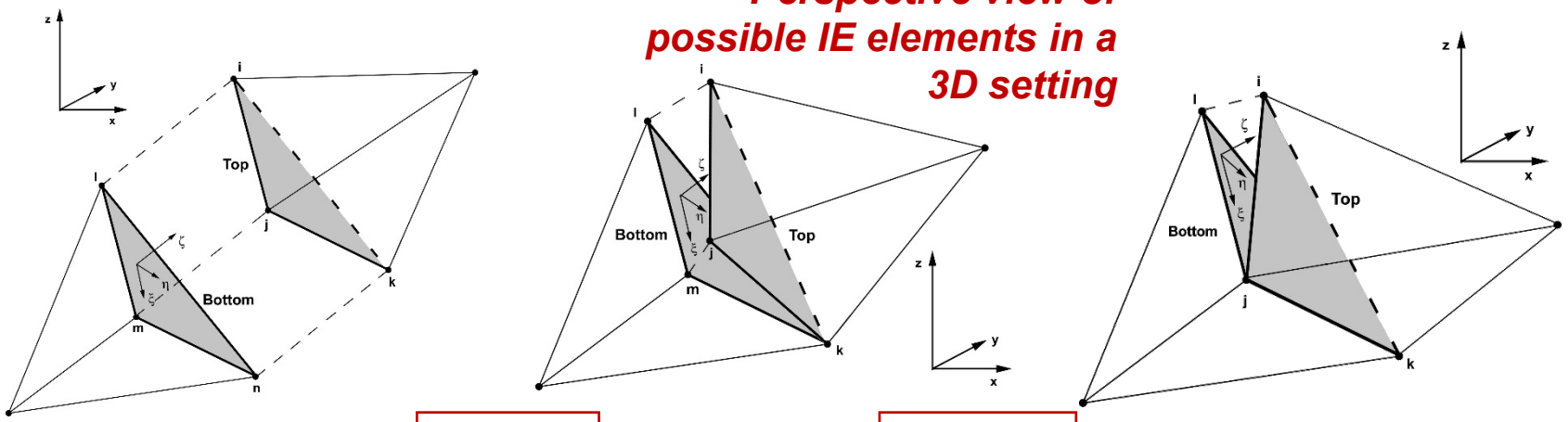

$\delta = Su$ $\quad$ $\sigma = D\delta$

TOP - BOTTOM IE displacements $[\mathbf{u}^{T,B} ; \mathbf{v}^{T,B}]$ → fault opening δ_n slippage δ_s → interface normal stress σ_n shear stress τ_s

Mohr-Coulomb Failure criterion:

$$\tau_L = c - \sigma_n \tan\varphi$$

Sealing or non-sealing faults

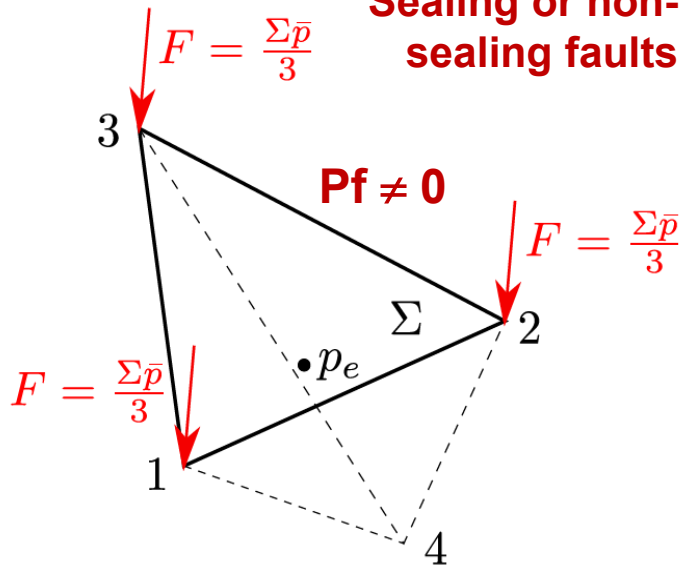

WP2 - Model set-up

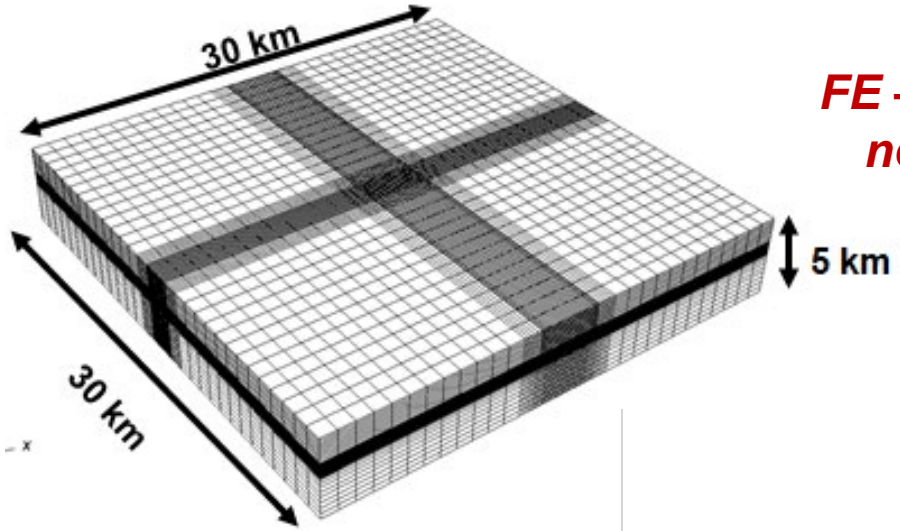

FE – IE mesh (253'165 nodes, 236'208 FEs, 5215 IEs)

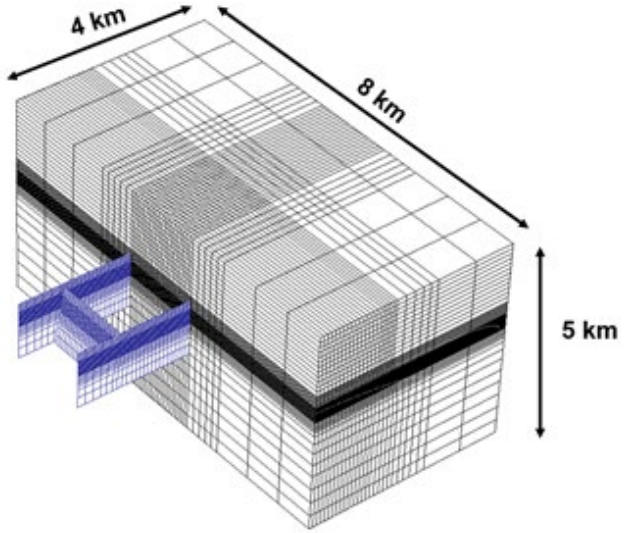

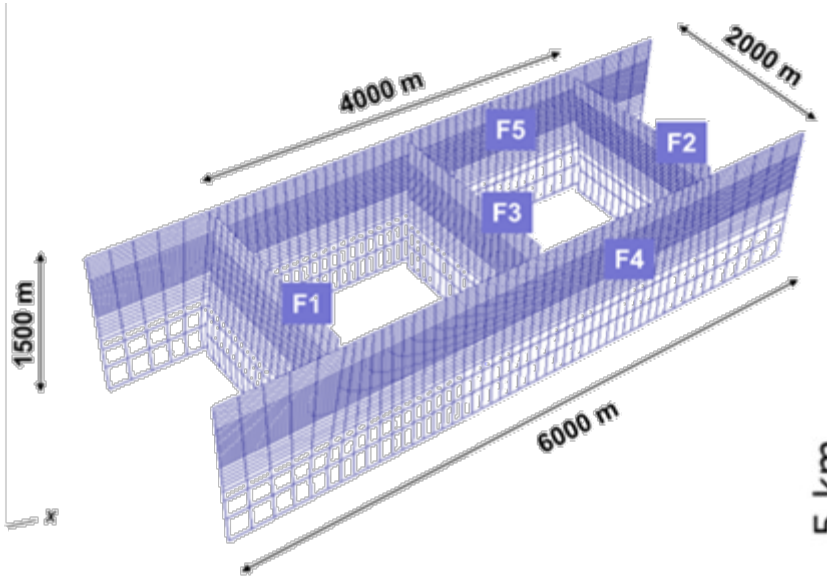

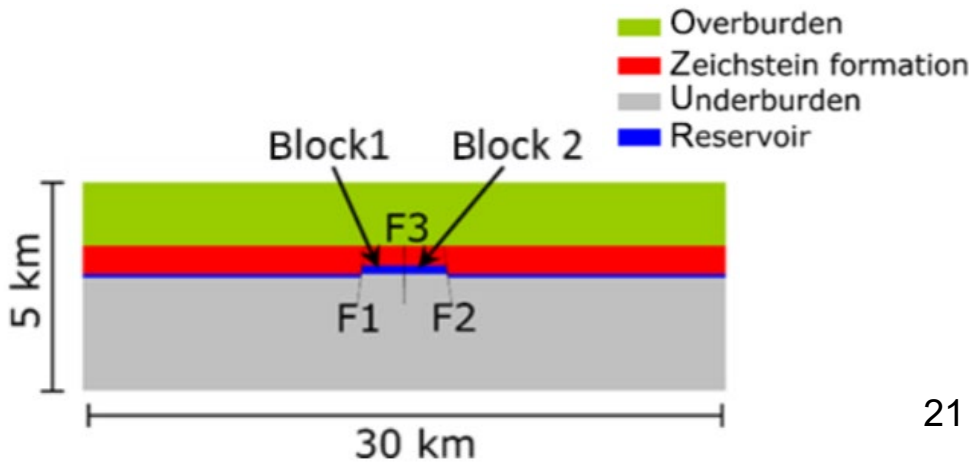

WP2 - Model set-up

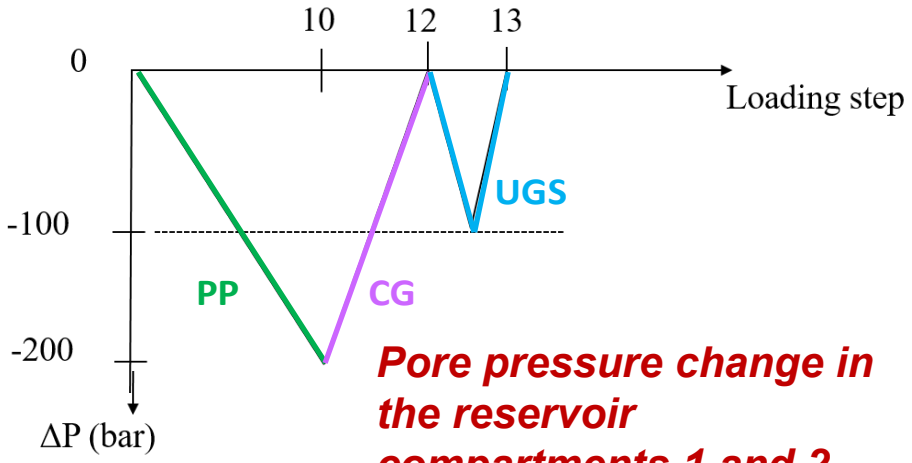

Pore pressure change in the reservoir compartments 1 and 2

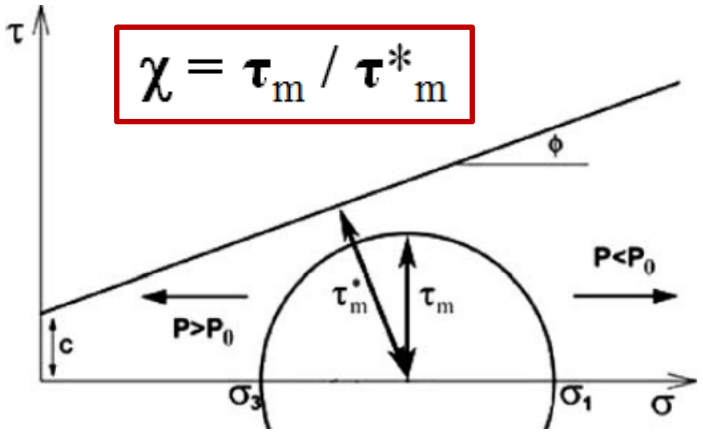

Mohr-Coulomb criterion with a criticality index χ

PARAMETER	VALUE	RANGES
F3 dip	90°	+65° – -65°
Dislocation	0 m	100 – 200 m
θ	0°	90°
M_1	0.74	0.42
M_2	0.83	0.45
Cohesion	20 bar	0 – 10 – 100 m bar
Static friction angle	30°	10° – 20° + weakening
$E_{reservoir}$	11 GPa	8 – 20 GPa
$E_{Zechstein < 1800 m}$	20 GPa	
$E_{Zechstein > 1800 m}$	35 GPa	
$E_{overburden}$	10 GPa	
$E_{underburden}$	30 GPa	
Zechstein	linear elastic	viscous (Maxwell $\mu = 10^{17}$ Pa·s)
α	0.86	1.0
$\nu_{reservoir}$	0.15	
$\nu_{Zechstein}$	0.30	
$\nu_{overburden}$	0.25	
$\nu_{underburden}$	0.20	
Pf	average between ΔP at the two sides of the fault	sealing Pf=0

Model parametrization for the "reference" and the investigated ranges

SIMULATED SCENARIOS

1) sensitivity to ΔPf (=0 → sealing ; 0.5(ΔP1+ ΔP2))
2) sensitivity to Biot's coefficient (1.0 instead of the actual value);
3) sensitivity to reservoir and fault geometry (F3 dip angles +65° and -65°, offset equal to 100 m and 200 m);
4) sensitivity to initial stress regime (θ=90°; M_1= 0.40 and M_2 = 0.47);
5) sensitivity to fault Mohr-Coulomb parameters (c=0 bar; φ_s=20°; φ_d=10° and d_c=2 mm; φ_d=20° and d_c=20 mm);
6) sensitivity to reservoir stiffness (E=8 bar; E=20 bar);
7) sensitivity to the differential pore pressure in the reservoir compartments (ΔP1= -100 bar and ΔP2 = 0 bar; ΔP1= -100 bar and ΔP2 = -200 bar);
8) sensitivity to caprock rheology (viscous instead of elastic).

+ COMBINATIONS (of previous simulated scenarios)

FAULT F3 GEOMETRY

a) dip angle = +65°
b) dip angle = –65°
c) dislocation = 100 m
d) dislocation = 200 m

Maximum elemental value of χ: comparison with the reference case

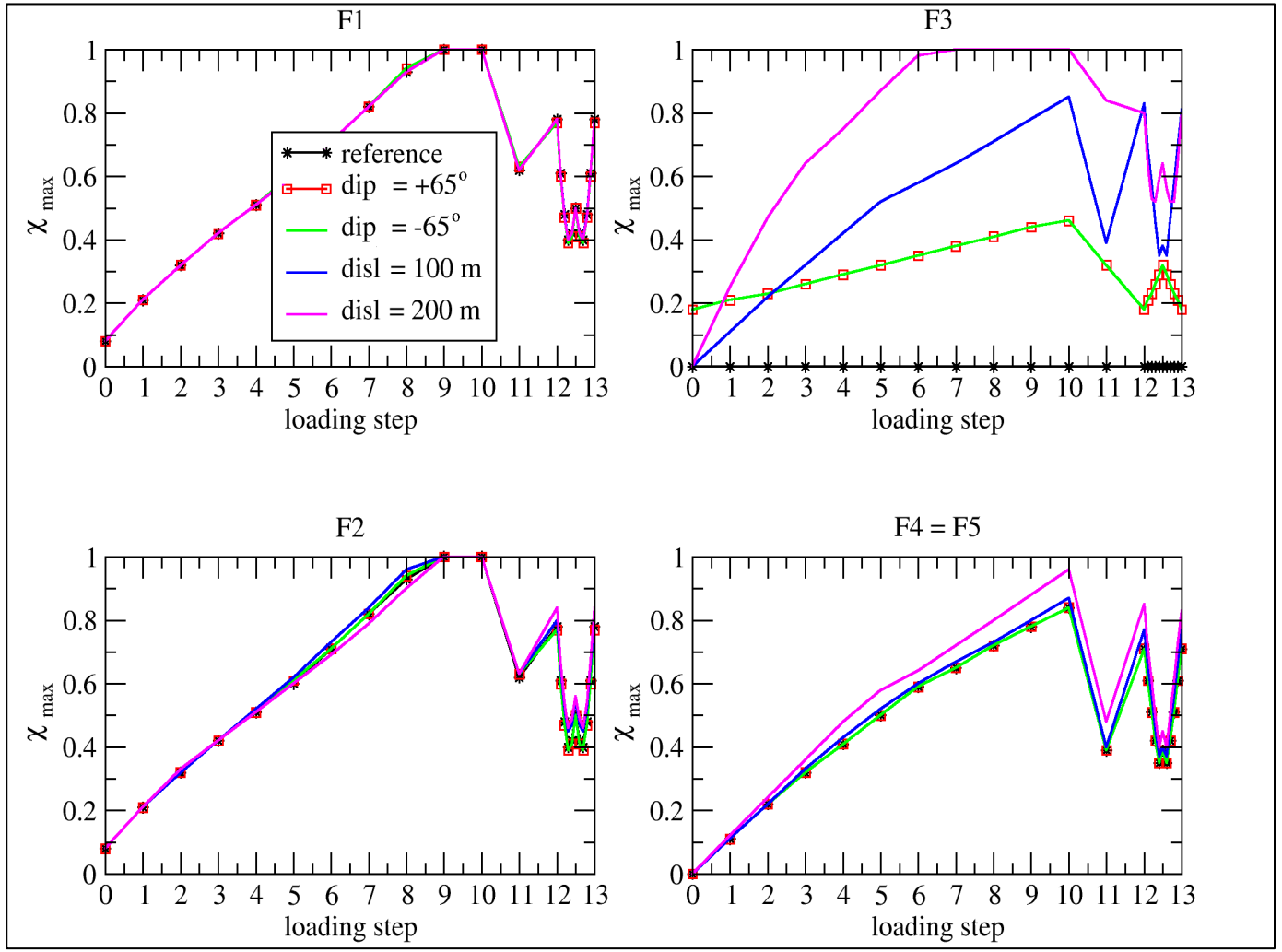

WP3-WP5-WP6 - Sensitivity & Scenarios

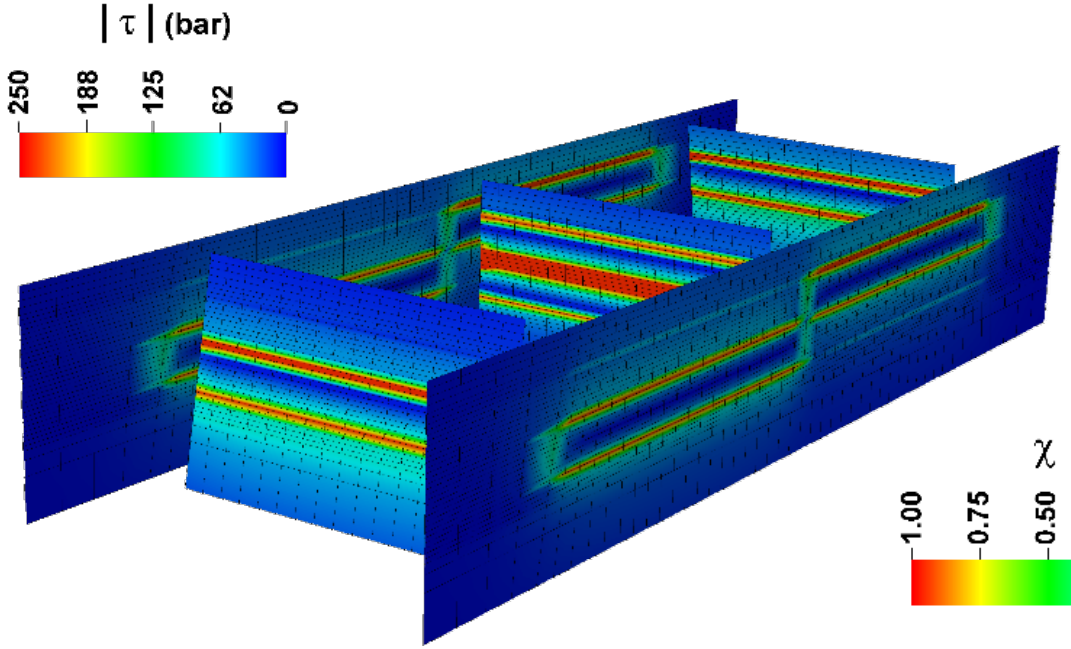

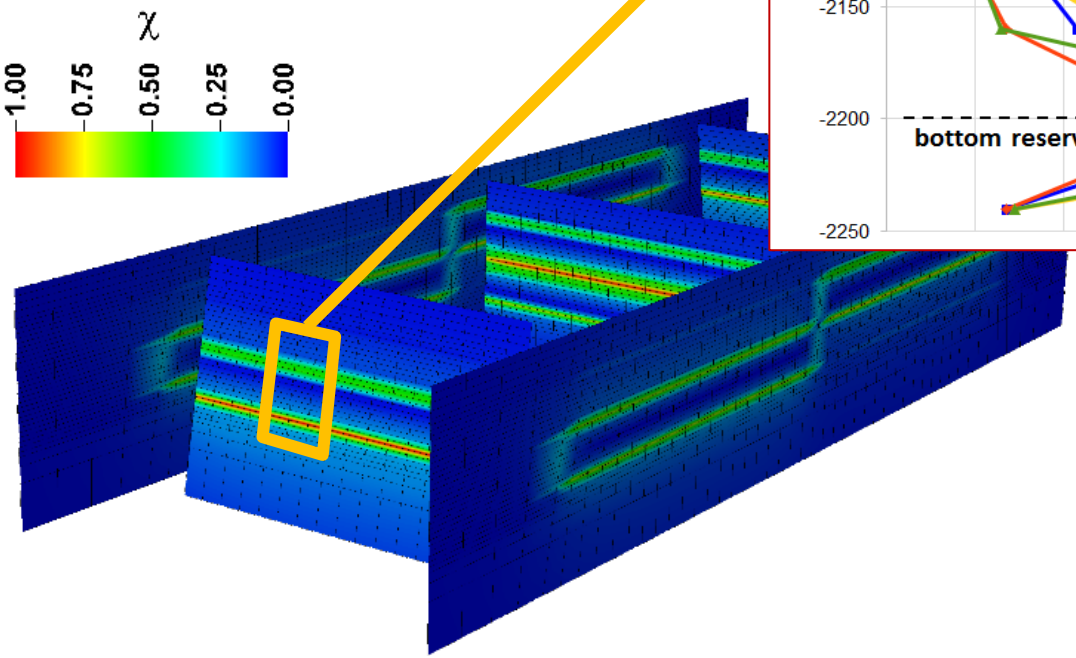

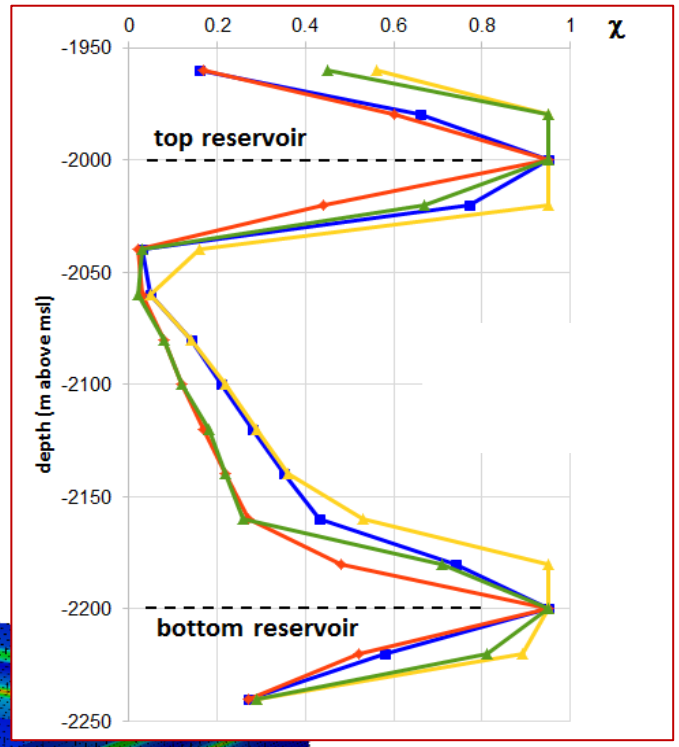

Scenario d: |τ| and (node-based) χ at the end of primary production

WP3-WP5-WP6 - Sensitivity & Scenarios

Fault activation during PP leads to a stress redistribution and a new (deformed) "equilibrated" configuration that is newly loaded, in the opposite direction, when the pressure variation changes the sign.

(a) Distribution of the shear stress τ for a few representative loading steps on fault F2 (dip = 10°).

(b) Time behavior of τ for the nodes shown in (a) located at the top (T), center (C), and bottom (B) of the reservoir.

(c) Sketches representing the reservoir deformation, shear stress direction, and inactive/active portions of the fault at the loading steps shown in (a).

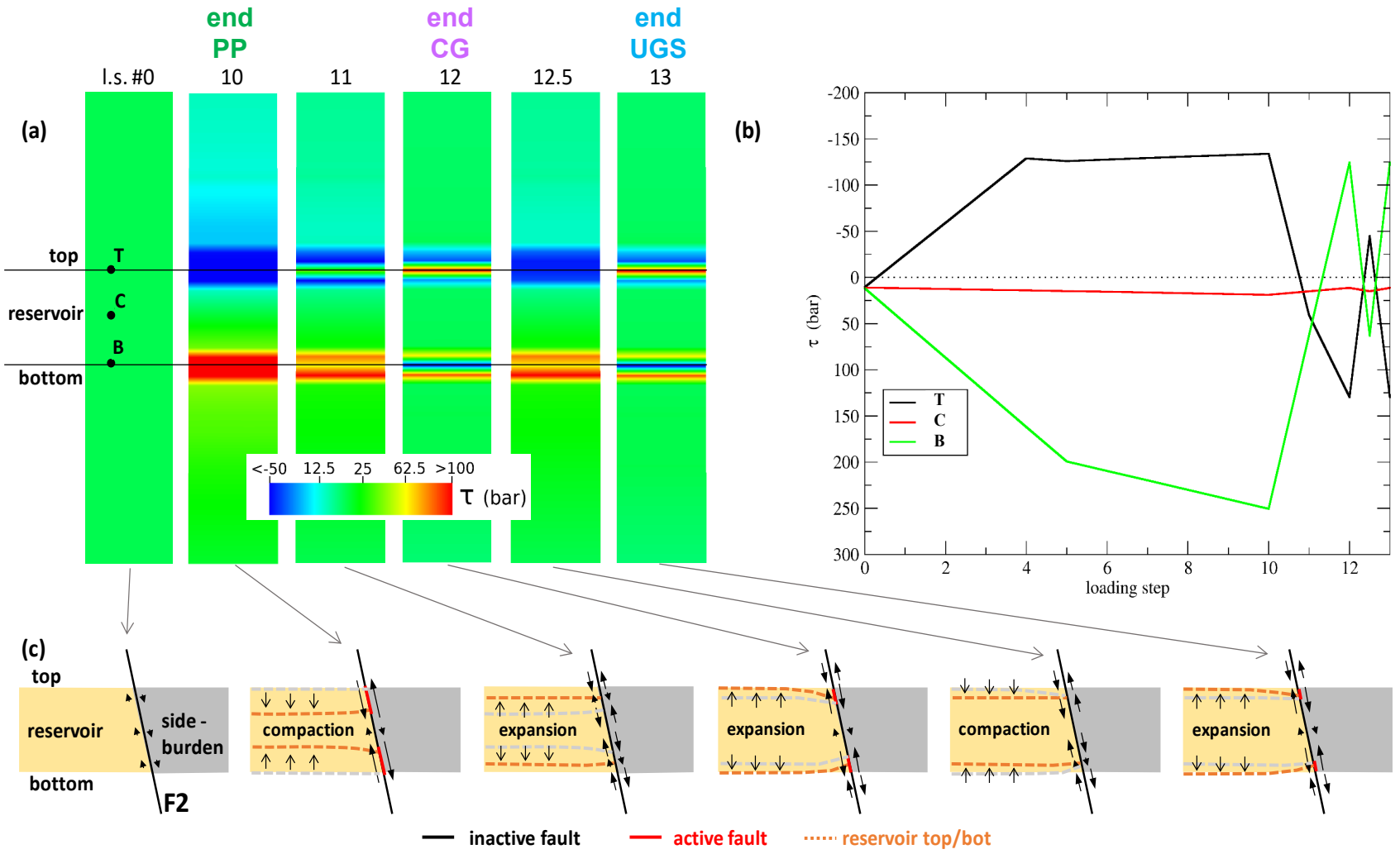

WP3-WP5-WP6 - Sensitivity & Scenarios

Scenarios a-d: maximum sliding δ_{max} versus time

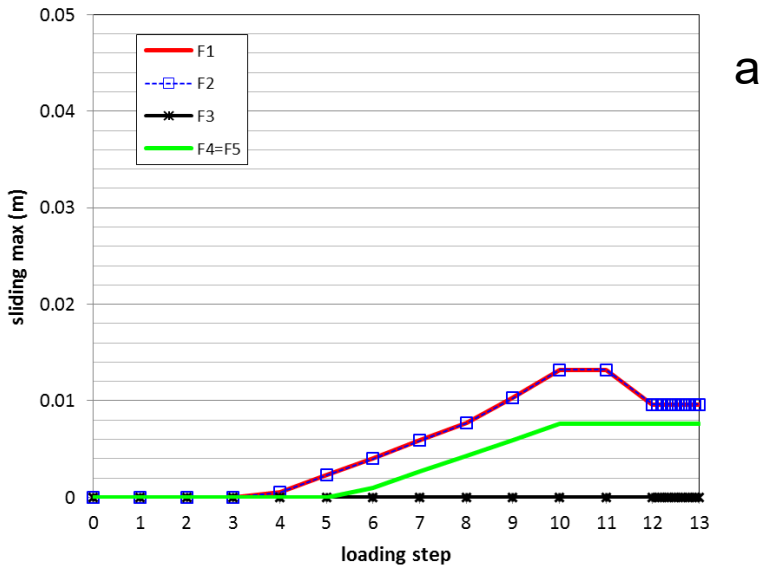

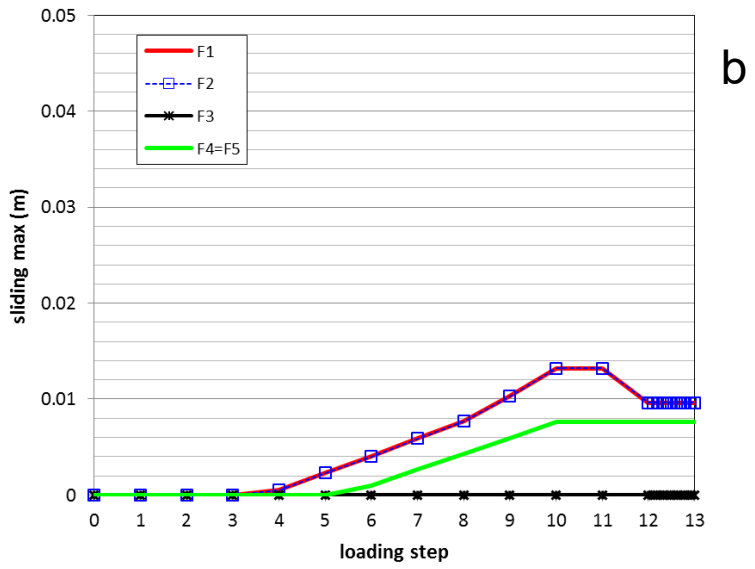

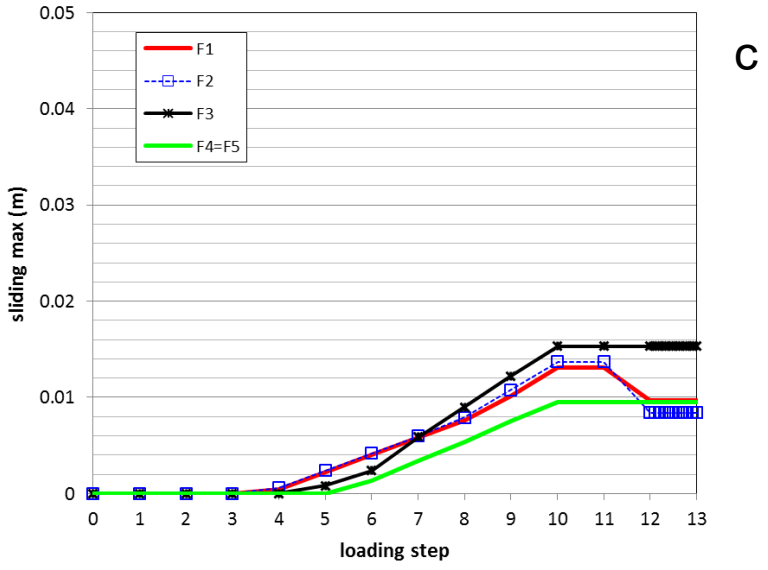

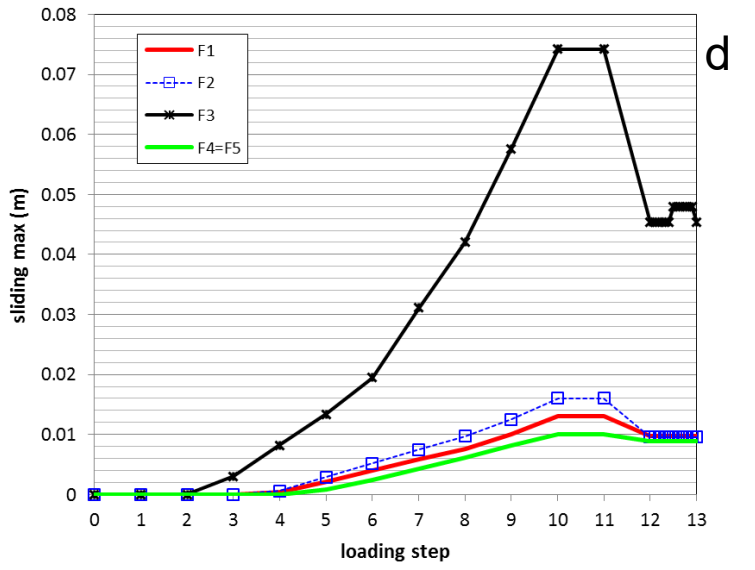

WP3-WP5-WP6 - Sensitivity & Scenarios

MOHR-COULOMB PARAMETERS

a) c = 0 bar
b) φ_s = 20°
c) φ_d = 10° and d_c = 2 mm
d) φ_d = 20° and d_c = 20 mm

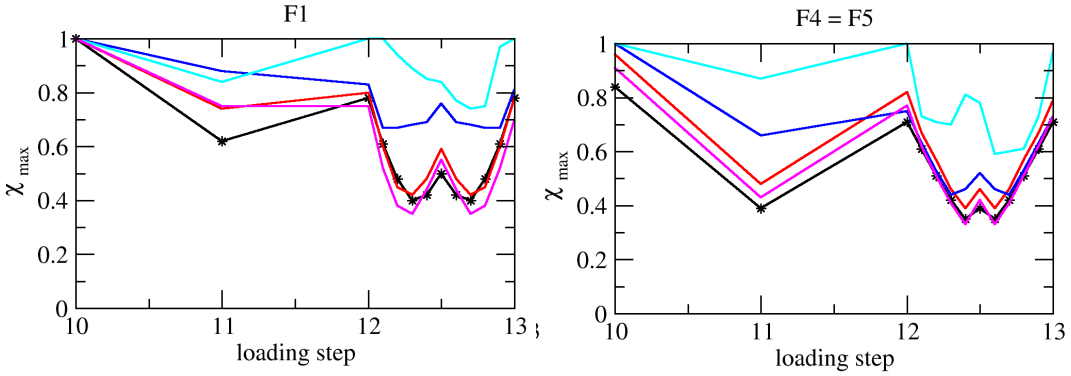

Maximum elemental value of χ: zoom over CG and UGS

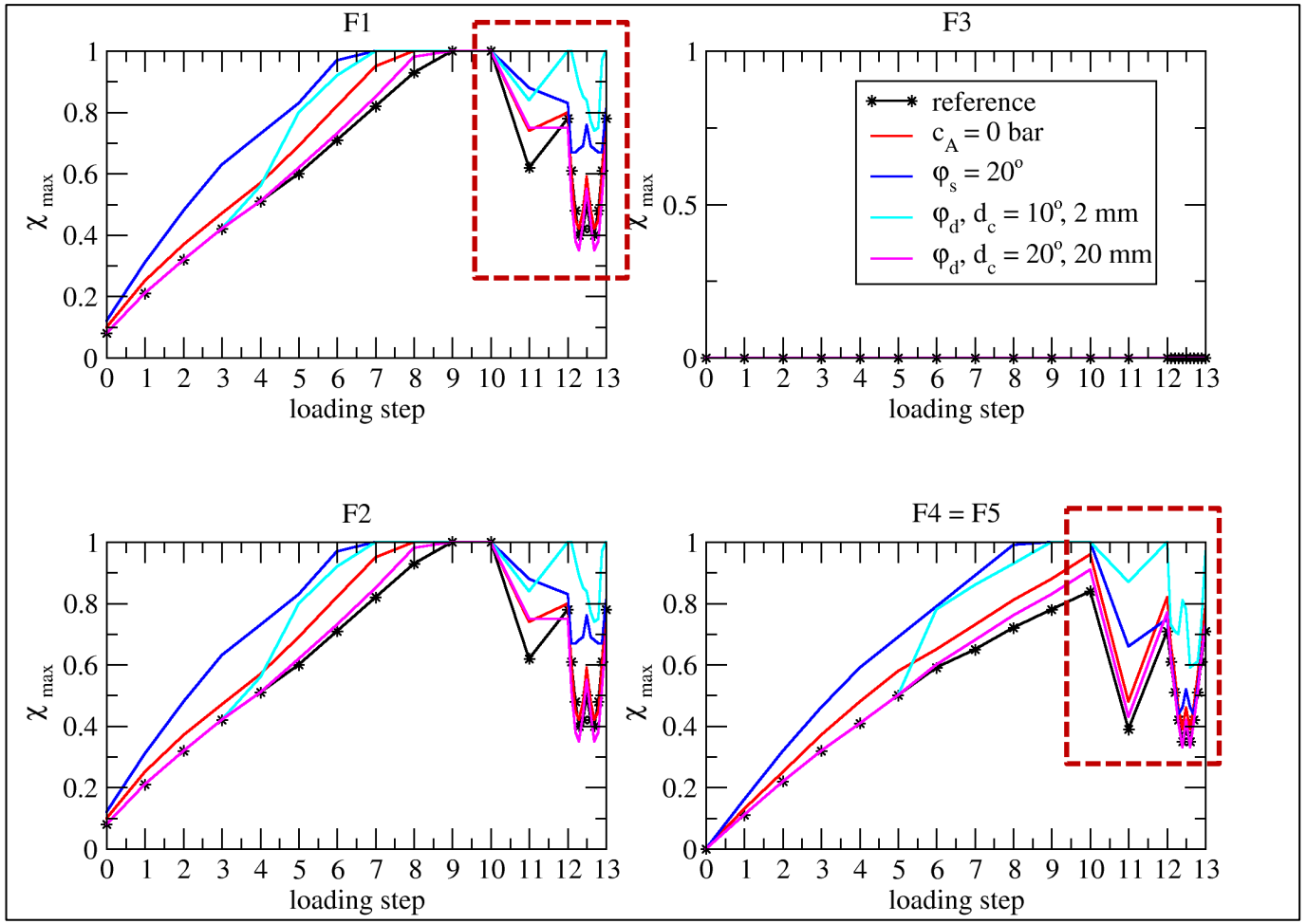

Maximum elemental value of χ: comparison with the reference case

WP3-WP5-WP6 - Sensitivity & Scenarios

Stress path |τ| vs σ for the F2 fault node 2665. The red line represents the yield bound and the numbers the various loading steps. Different colours are used for primary production (PP, loading steps #1 – 10), cushion gas (CG, loading steps #11 – 12), and underground gas storage (UGS, loading steps #12.1 – 13).

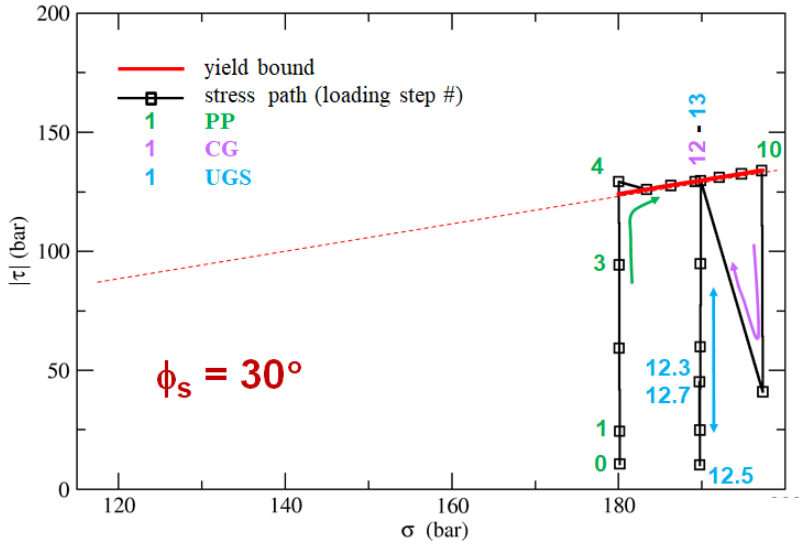

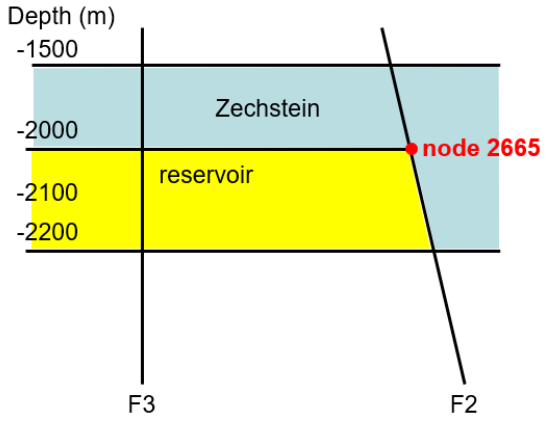

Location of the node used to represent the stress path

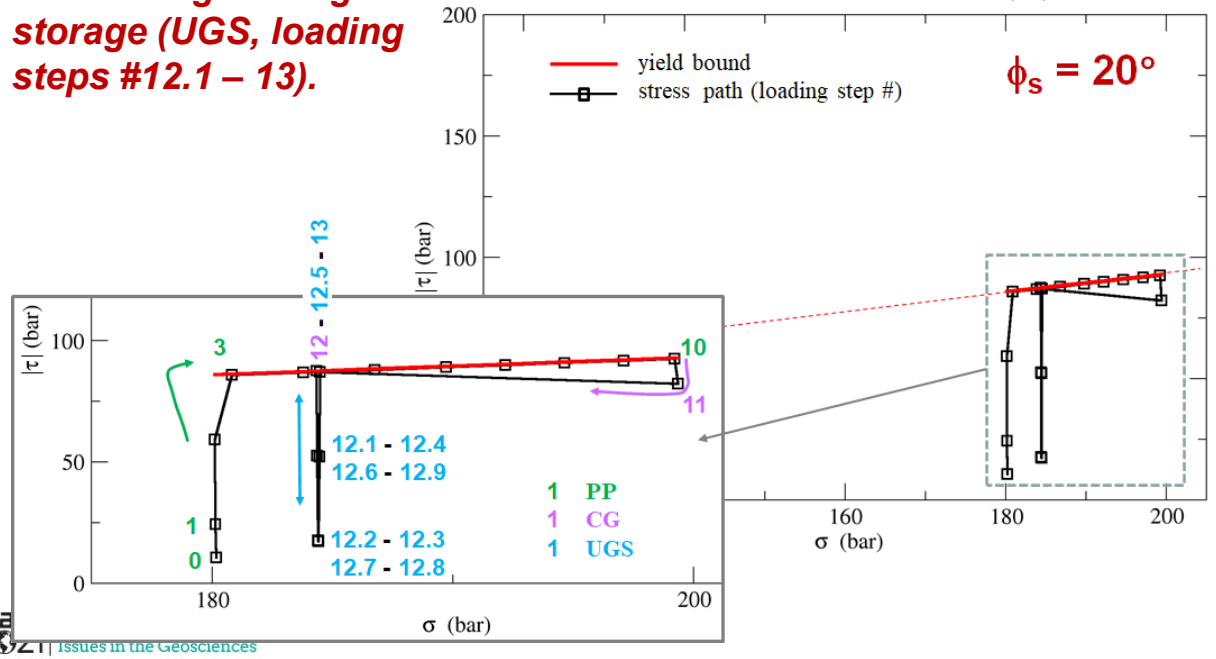

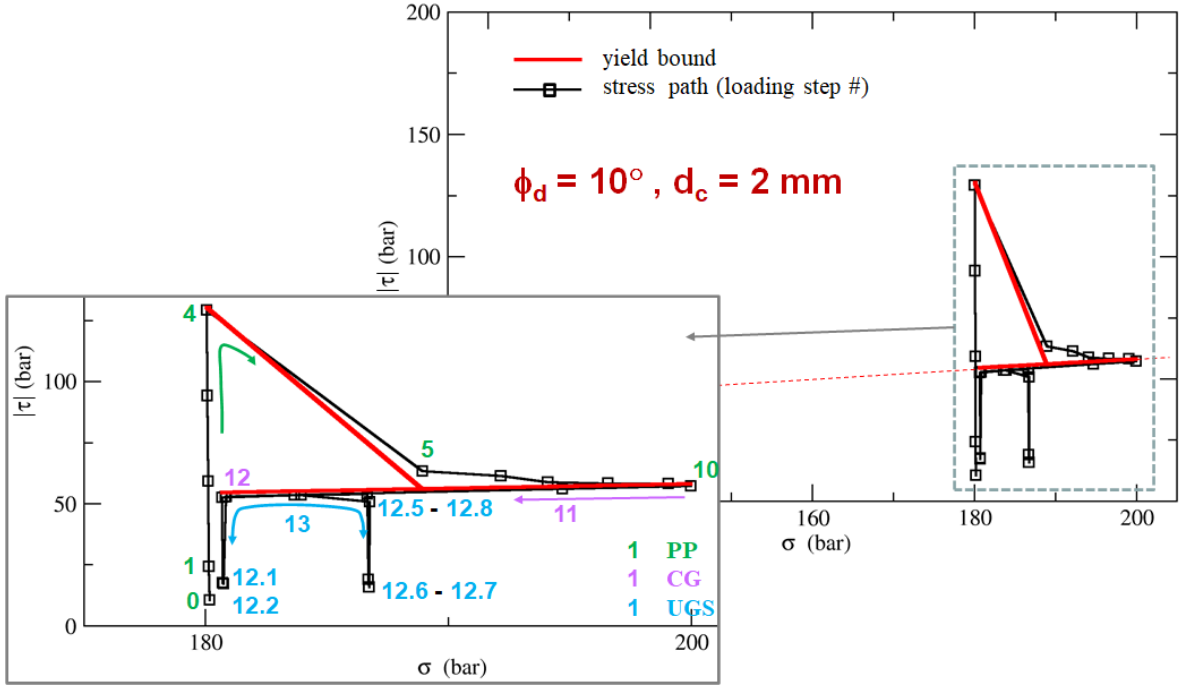

MOST CRITICAL COMBINATION

- static friction angle = 20°;
- F3 dip angle = +65°;
- viscous caprock;
- compartment offset = 100 m
- other parameters: reference case

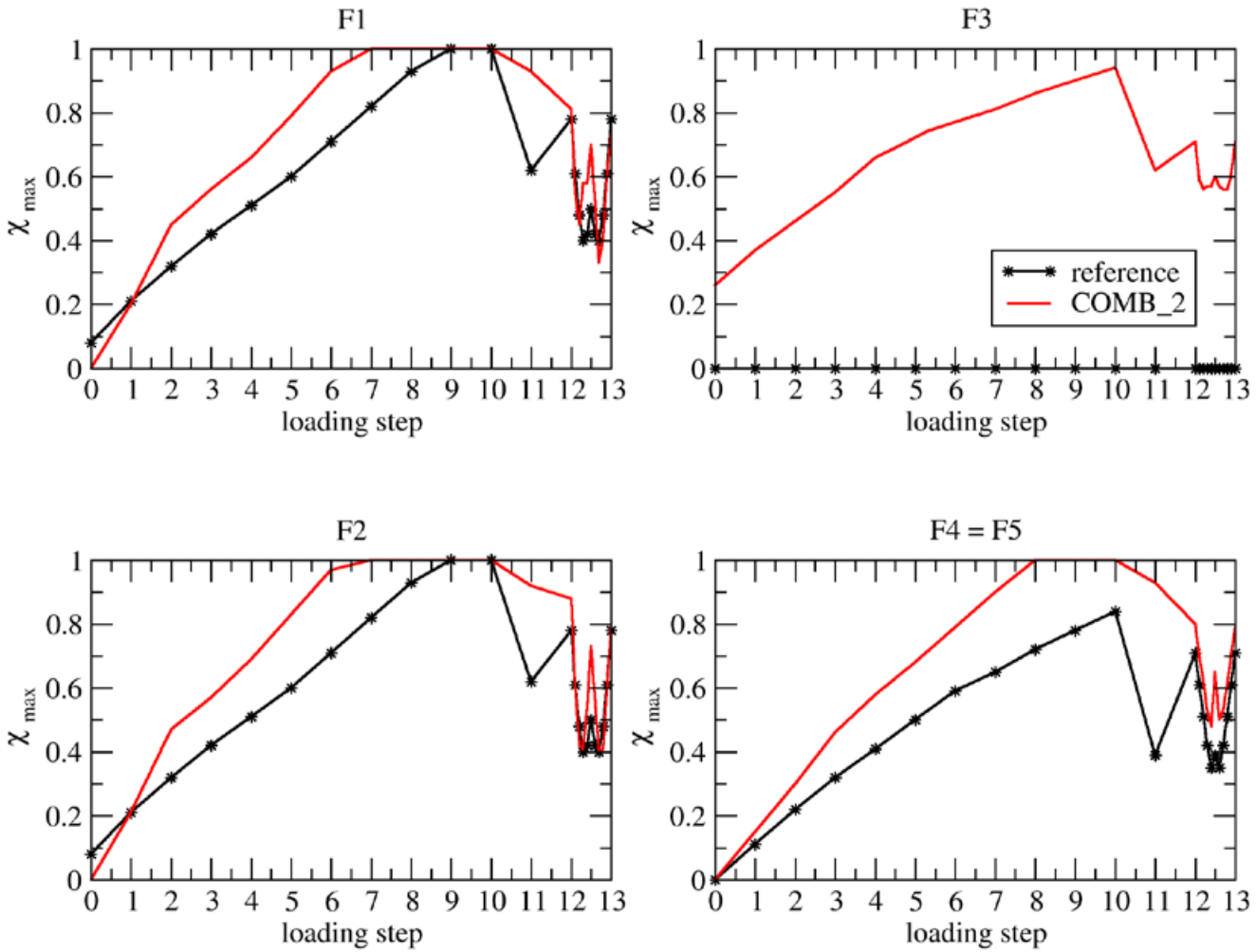

Maximum elemental value of χ: comparison with the reference case

WP3-WP5-WP6 - Sensitivity & Scenarios

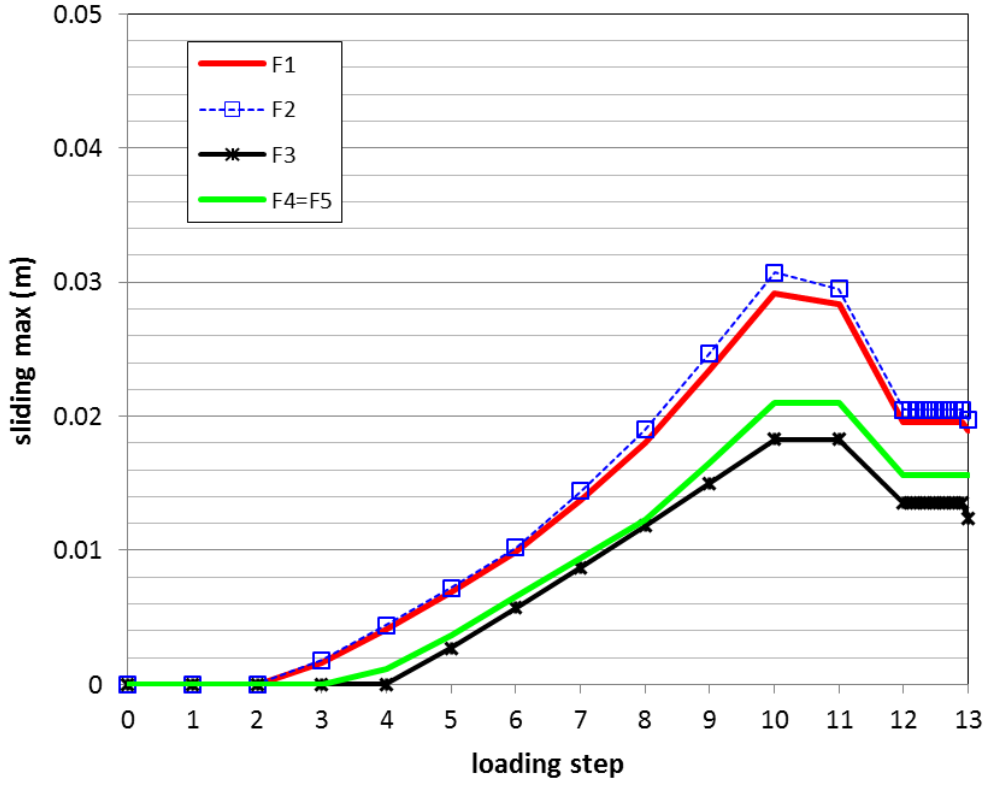

Maximum sliding δ_{max} versus time

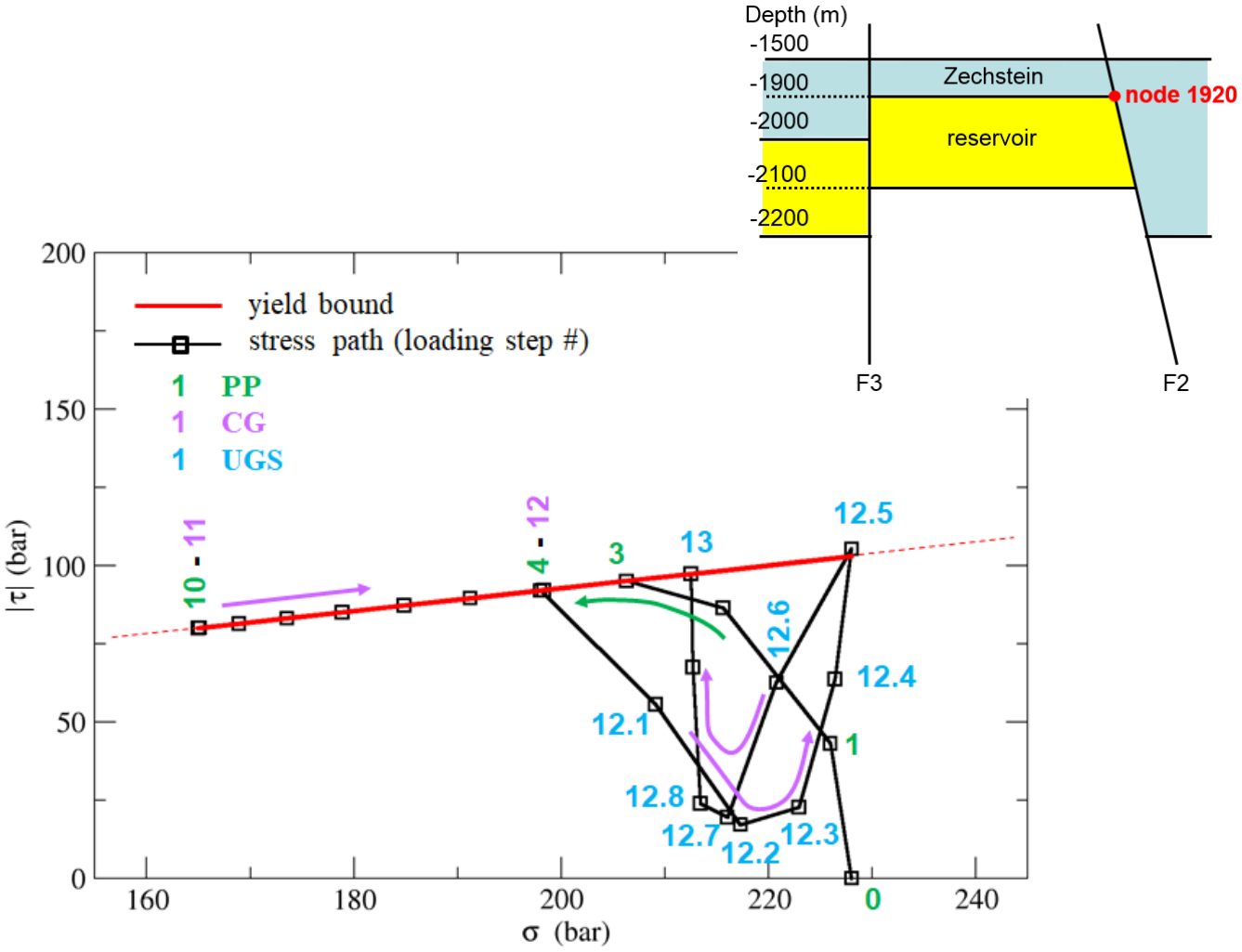

Stress path |τ| vs σ for the F2 fault node 1920

WP4-WP7 - Comparing scenarios

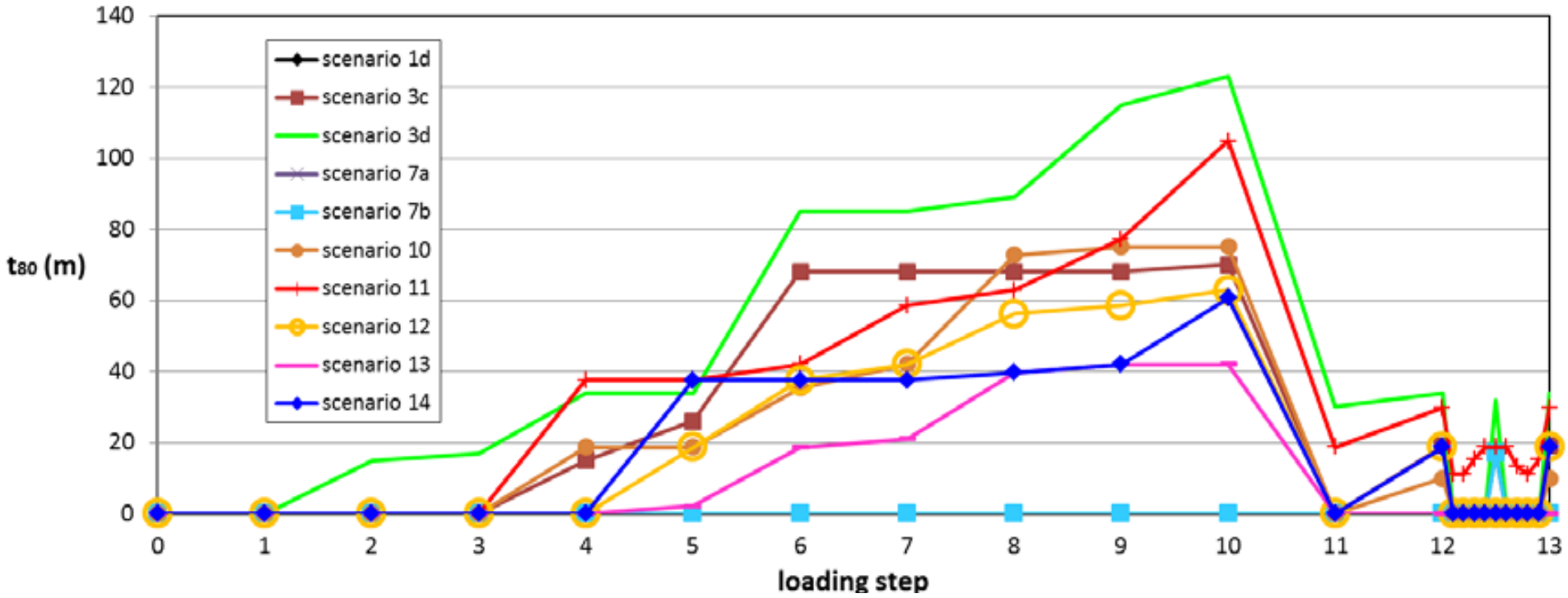

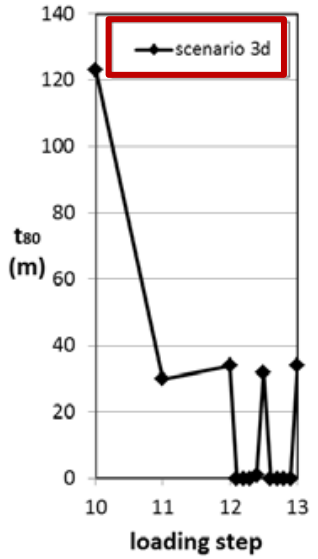

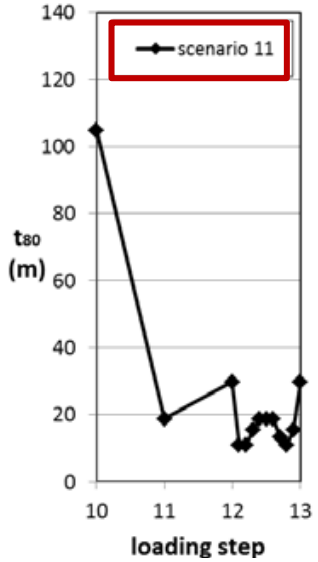

t_{80} time behaviors obtained for fault F3 for scenarios with asymmetry in the geological setting and/or stress driving forces

WP4-WP7 - Ranking scenarios

Scenarios are ranked following these nested criteria:

- (a) element-based χ_{max} during UGS; or (b) $\chi^* = \Sigma_{element}(t_e \cdot \chi|_{\chi>0.8})$ normalized over $\max(\chi^*)|_{scenarios}$ where t_e is the element thickness (more generally the element area if a non-regular discretization is used);
- maximum value of average sliding (δ_{avg}), evaluated on active elements only;
- loading step of activation.

Scenario #	Parameter / Mechanism	χ_{max} UGS	Maximum δ_{avg}	Activation L.S.	χ_{max}
5c	φ_d = 10° ; d_c = 2 mm	1.00	0.026	7	1
7b	ΔP1 = -100 bar; ΔP2 = -200 bar	0.97	0.010	9	1
4b	M1-M2 lower	0.96	0.018	6	1
3d	disl = 200 m	0.84	0.008	9	1
5b	φ_s = 20°	0.81	0.010	7	1
3c	disl = 100 m	0.80	0.007	9	1
6a	E = 8 GPa	0.79	0.010	8	1
5a	c = 0 bar	0.78	0.008	8	1
7a	ΔP1 = -100 bar; ΔP2 = 0 bar	0.78	0.007	9	1
8	UGS ΔP1 = ΔP2 = -150 bar	0.78	0.007	9	1
3a/b	F3 dip = 65°	0.77	0.007	8	1
2	Biot = 1.0	0.76	0.008	8	1
4a	θ = 90°	0.74	0.007	10	1
9	viscous salt caprock	0.70	0.009	10	1
5d	φ_d = 20° ; d_c = 20 mm	0.70	0.009	8	1
6b	E = 20 Gpa	0.78	0.005	-	0.79

Scenario #	Parameter / Mechanism	χ^*	Maximum δ_{avg}	Activation L.S.	χ_{max}
4b	M1-M2 lower	1.00	0.018	6	1
5c	φ_d = 10° ; d_c = 2 mm	0.62	0.026	7	1
7b	ΔP1 = -100 bar; ΔP2 = -200 bar	0.52	0.010	9	1
5b	φ_s = 20°	0.51	0.010	7	1
8	UGS ΔP1 = ΔP2 = -150 bar	0.39	0.007	9	1
5a	c = 0 bar	0.29	0.008	8	1
6a	E = 8 GPa	0.27	0.010	8	1
3d	disl = 200 m	0.26	0.008	9	1
3c	disl = 100 m	0.26	0.007	9	1
7a	ΔP1 = -100 bar; ΔP2 = 0 bar	0.26	0.007	9	1
3a/b	F3 dip = 65°	0.26	0.007	8	1
2	Biot = 1.0	0.25	0.008	8	1
5d	φ_d = 20° ; d_c = 20 mm	0.23	0.009	8	1
4a	θ = 90°	0.22	0.007	10	1
9	viscous salt caprock	0.17	0.009	10	1
6b	E = 20 GPa	0.17	0.005	-	0.79

BOUNDING FAULT

WP4-WP7 - Ranking scenarios

Scenario #	Parameter / Mechanism	χ_{max} UGS	Maximum δ_{avg}	Activation L.S.	χ_{max}
3d	disl = 200 m	0.84	0.033	7	1
3c	disl = 100 m	0.81	0.007	-	0.85
7a	ΔP1 = -100 bar; ΔP2 = 0 bar	0.53	0.000	-	0.53
7b	ΔP1 = -100 bar; ΔP2 = -200 bar	0.53	0.000	-	0.53
3a/b	F3 dip = 65°	0.32	0.000	-	0.46
2	Biot	0.00	0.000	-	0
4a	theta = 90°	0.00	0.000	-	0
4b	M1-M2 lower	0.00	0.000	-	0
5a	c = 0 bar	0.00	0.000	-	0
5b	φ_s = 20°	0.00	0.000	-	0
5c	φ_d = 10° ; d_c = 2 mm	0.00	0.000	-	0
5d	φ_d = 20° ; d_c = 20 mm	0.00	0.000	-	0
6a	E = 8 GPa	0.00	0.000	-	0
6b	E = 20 GPa	0.00	0.000	-	0
8	UGS ΔP1 = ΔP2 = -150 bar (mech 04)	0.00	0.000	-	0
9	salt caprock	0.00	0.000	-	0

Scenario #	Parameter / Mechanism	χ^*	Maximum δ_{avg}	Activation L.S.	χ_{max}
3d	disl = 200 m	1.00	0.033	7	1
3c	disl = 100 m	0.71	0.007	-	0.85
3a/b	F3 dip = 65°	0.50	0.000	-	0.46
7b	ΔP1 = -100 bar; ΔP2 = -200 bar	0.31	0.000	-	0.53
7a	ΔP1 = -100 bar; ΔP2 = 0 bar	0.29	0.000	-	0.53
2	Biot	0.00	0.000	-	0
4a	theta = 90°	0.00	0.000	-	0
4b	M1-M2 lower	0.00	0.000	-	0
5a	c = 0 bar	0.00	0.000	-	0
5b	φ_s = 20°	0.00	0.000	-	0
5c	φ_d = 10° ; d_c = 2 mm	0.00	0.000	-	0
5d	φ_d = 20° ; d_c = 20 mm	0.00	0.000	-	0
6a	E = 8 GPa	0.00	0.000	-	0
6b	E = 20 GPa	0.00	0.000	-	0
8	UGS ΔP1 = ΔP2 = -150 bar (mech 04)	0.00	0.000	-	0
9	salt caprock	0.00	0.000	-	0

INTRA-RESERVOIR FAULT

Faults bounding the reservoir

During UGS the stability is manly jeopardized by:

- an **initial stress regime** with small horizontal principal components,
- failure criterion with **low friction angle**,
- **large pressure change** because of production/injection,
- significant **contrast** between the reservoir and the over- side- and underburden **stiffness**.

Intra-reservoir faults

During UGS the stability is manly jeopardized by:

- **dislocation** of the reservoir compartments,
- **different pressure change** in the two compartments,
- **fault dip**.

WP4-WP7 - Guidelines for safe operational bandwidths

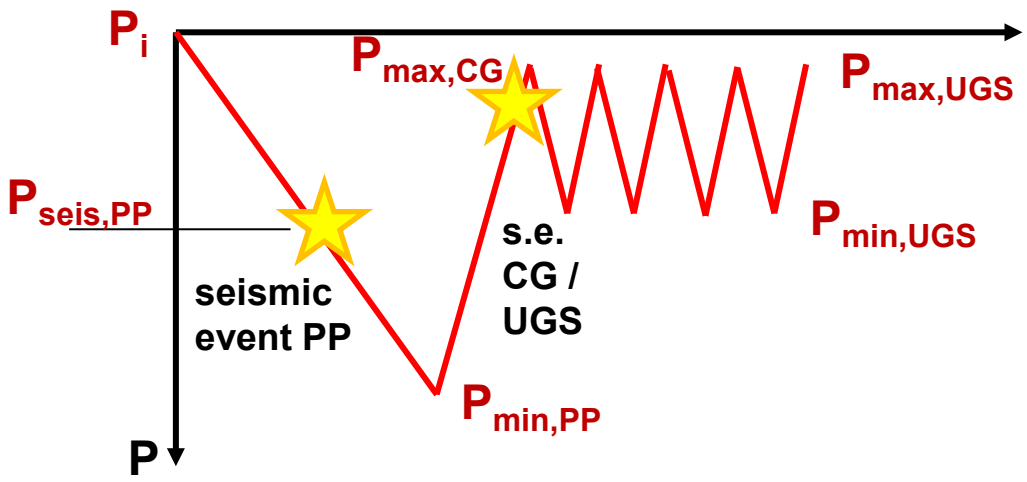

The numerous scenarios investigated within the study have clearly revealed that fault reactivation can occur during CG and UGS, more likely if :

i) **seismicity has been recorded during PP and**
ii) **when the reservoir pressure is approaching or reaches $P_{max,CG}$, $P_{max,UGS}$, and $P_{min,UGS}$.**

A few **qualitative guidelines** have been produced to bound $P_{max,CG}$, $P_{max,UGS}$, and $P_{min,UGS}$ **depending on** $P_{seis,PP}$ and $P_{min,PP}$

WP4-WP7 - Guidelines for safe operational bandwidths

- If seismicity has been recorded during PP, $P_{max,CG}$ and $P_{max,UGS}$ must be smaller than P_i; a rough rule could be to keep the pressure recovery smaller than:

$$\min[\theta|P_i - P_{seis,PP}| \; ; \; |P_i - P_{min,PP}| \;] \; , \; 1 \leq \theta \leq 2$$

  - $P_{min,PP} << P_{seis,PP}$
  - $P_{min,PP} \sim P_{seis,PP}$

- if seismicity has been recorded during PP, $P_{min,UGS}$ must be larger than $P_{min,PP}$; a rough rule could be to keep $P_{min,UGS}$ larger than the reservoir pressure at the time of seismic occurrence;

- if seismicity has been recorded during PP, avoid during CG and UGS to cause a pressure change between various reservoir compartments larger than that at the time of seismic occurrence;

- if no seismicity has been recorded during PP, $P_{max,CG}$ can safely be equal to P_i;

- if no seismicity has been recorded during PP and CG, UGS pressure change can safely span the whole pressure change between P_i and $P_{min,PP}$.

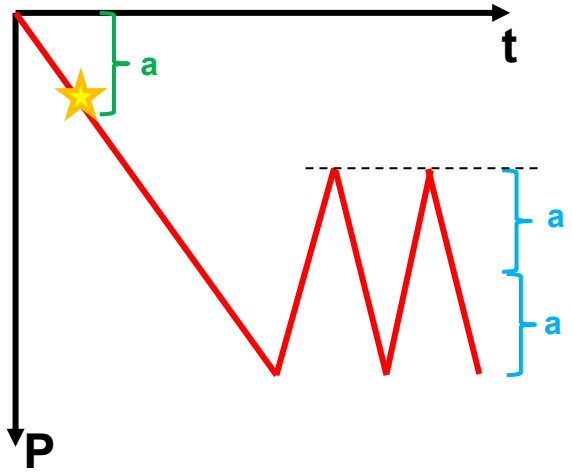

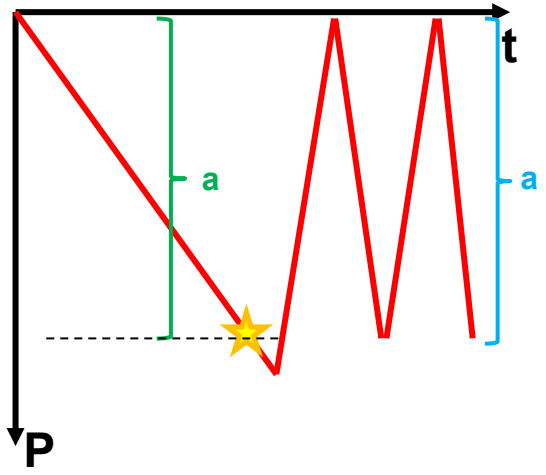

SEISMIC DATA ASSIMILATION IN GEOMECHANICAL MODELING

- Sensitivity analysis via Sobol' indices
- Bayesian update of FE-IE geomechanical model (MCMC)
- Forward full model is approximate via surrogate solution (generalized polynomial chaos expansion)
- Assimilation of seismic moment M_0
- N = 5000 realizations
- Effective constrain of parameters τ_0 and M_2

Surrogate vs forward model outcomes

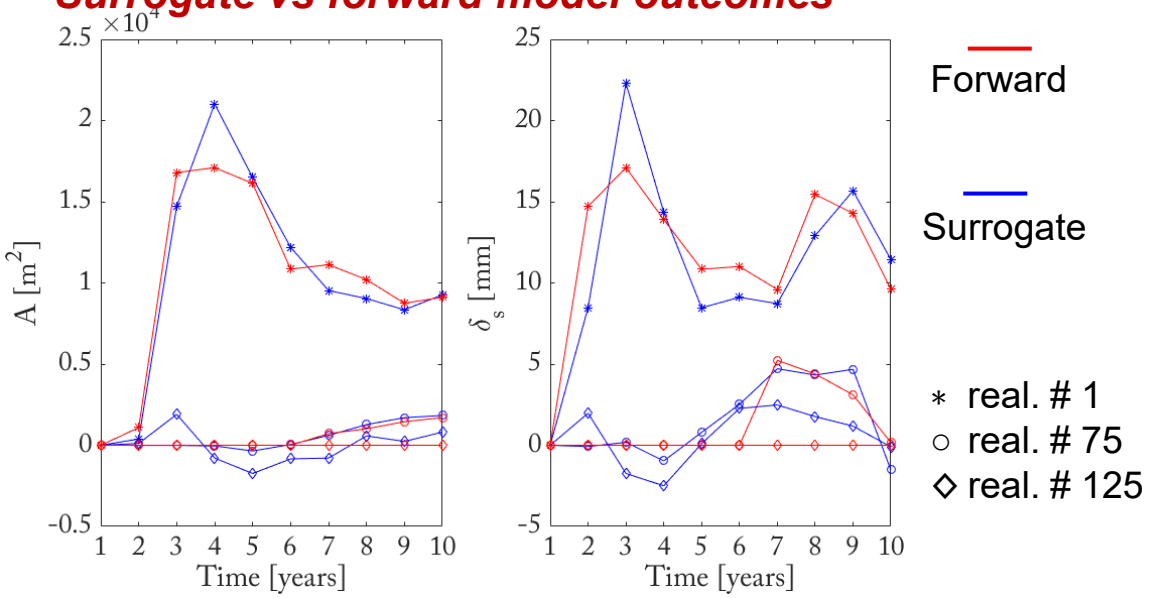

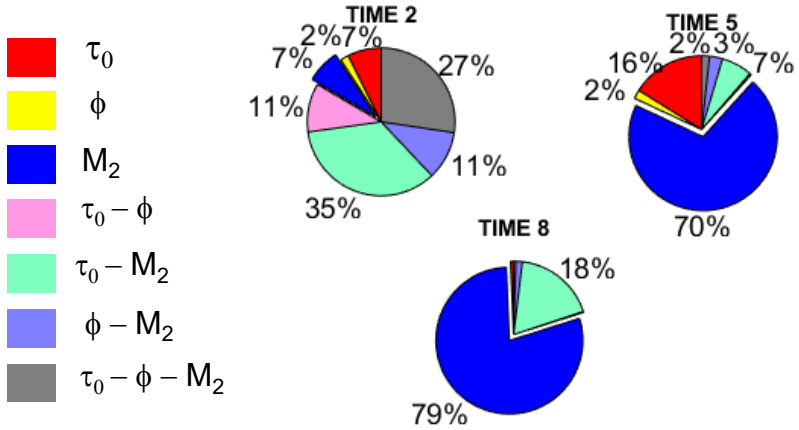

Sensitivity analysis

Prior and POSTERIOR cumulative DISTRIBUTIONS of τ_0, ϕ, M_2

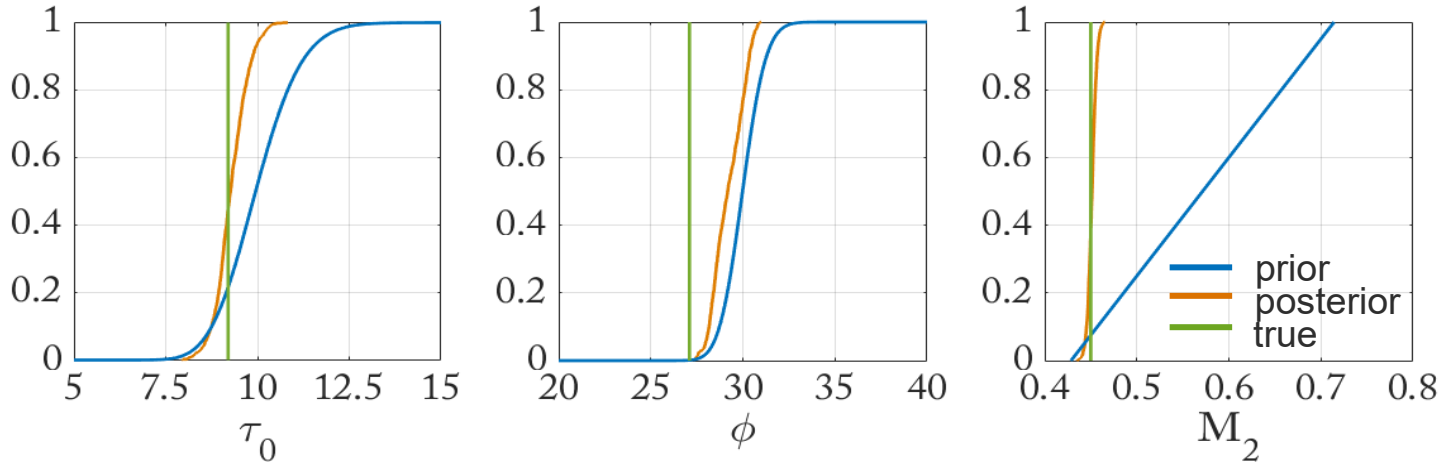

MODEL APPROXIMATIONS BY ML TECHNIQUES

- ***Gradient boosting tree:*** machine learning technique, an ensemble-based tree method
- Investigations of the relationship between a set of input combinations and output space
- Application to ground ruptures due to the excessive groundwater pumping
- Analysis of relative importance of geometry, compressibility, pore pressure

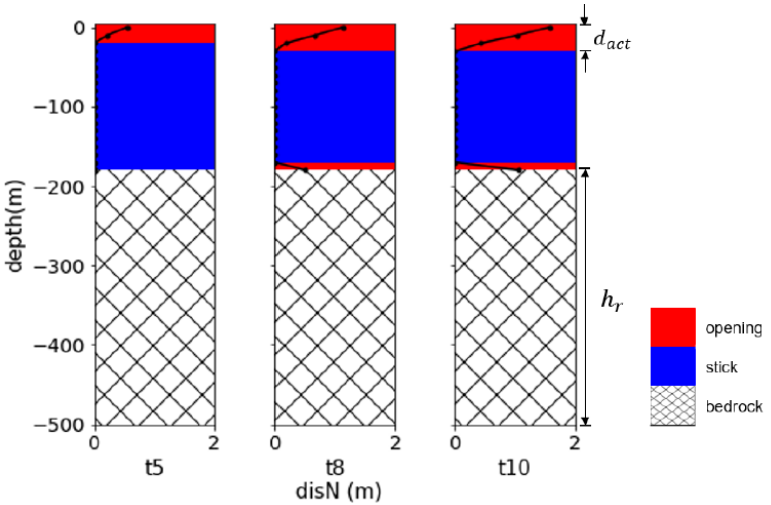

Sequential evolution of fissure for the 5th, 8th and 10th loading steps

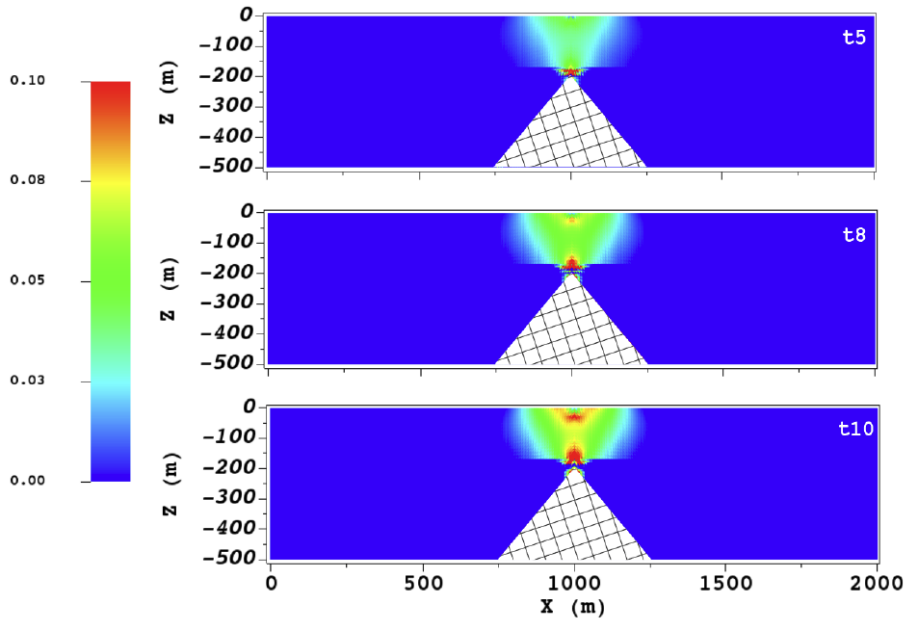

Sequential evolution of dimensionless horizontal stress for the 5th, 8th and 10th loading steps

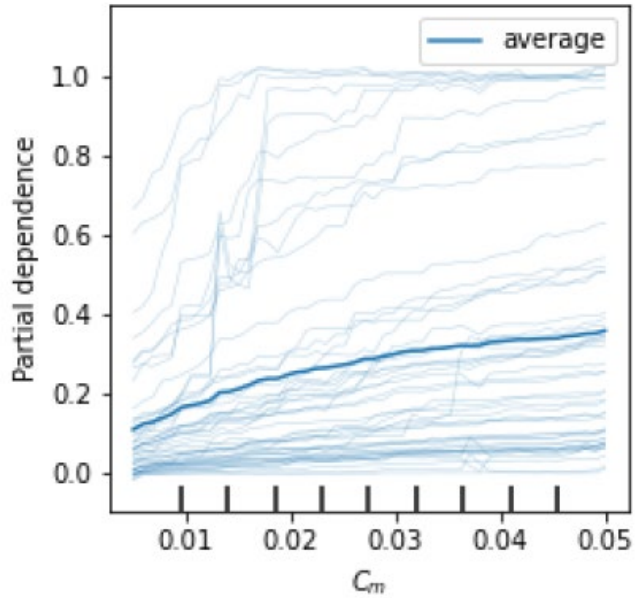

Individual conditional expectation for the aquifer C_m

COUPLED MODEL OF CONTACT MECHANICS AND FLUID FLOW: PENNY-SHAPED CRACK

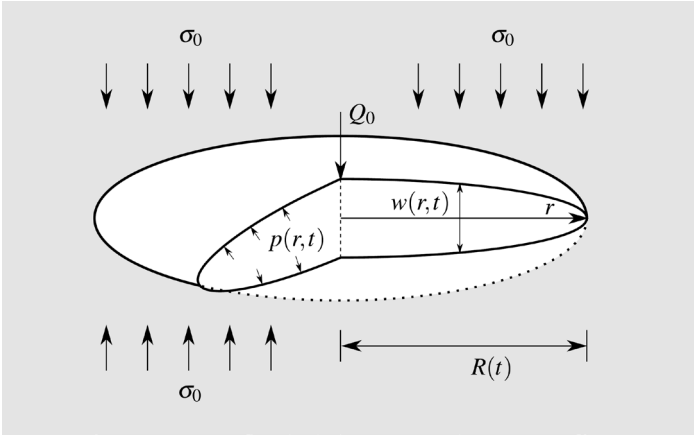

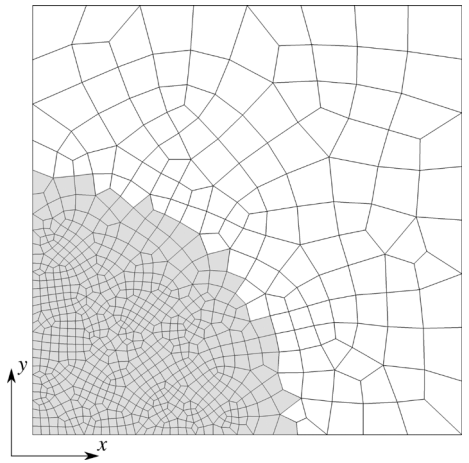

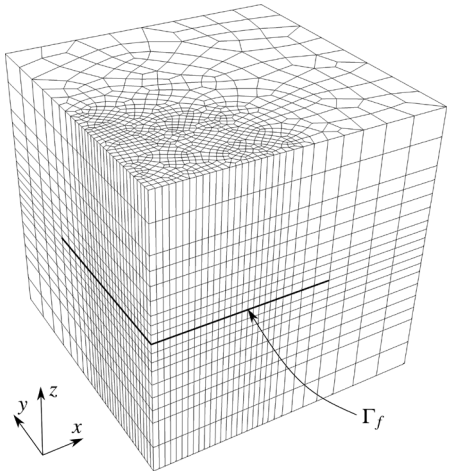

Sketch and mesh used in the analytical 3D example with flow

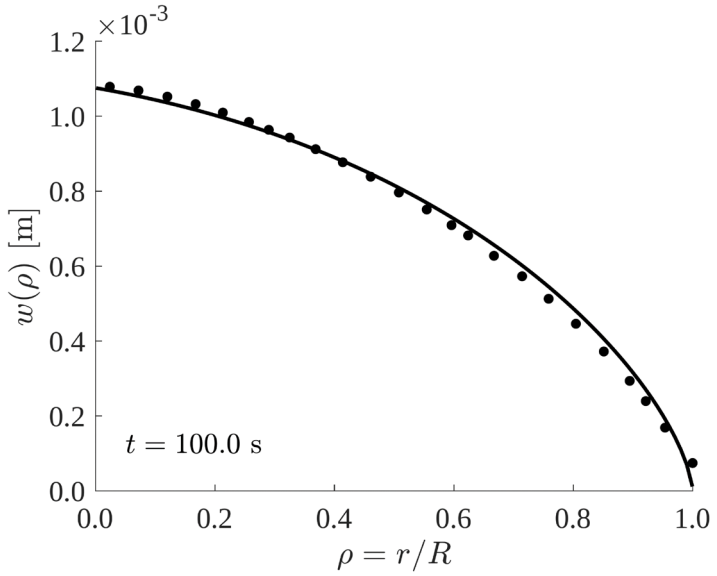

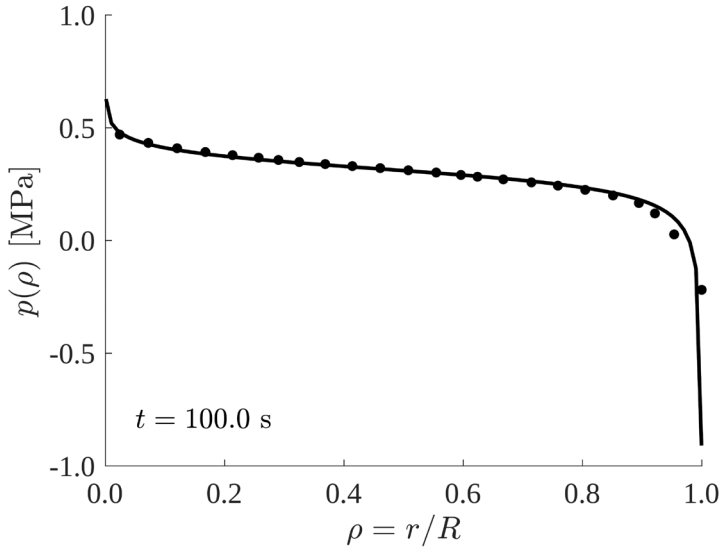

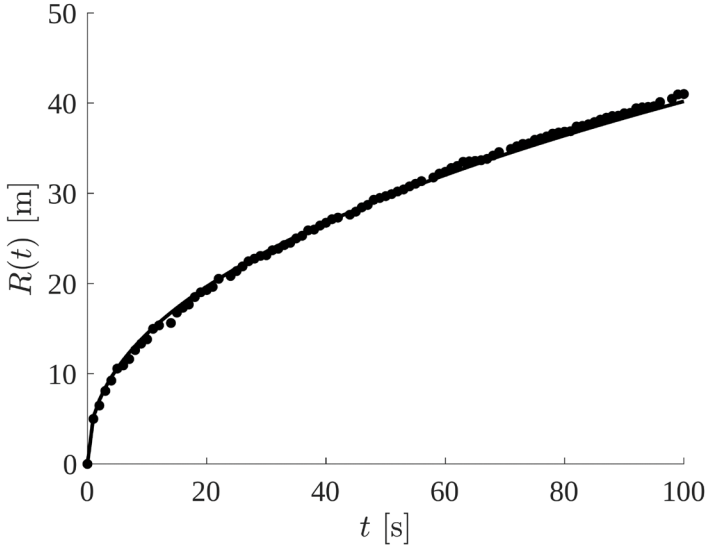

Comparison in terms of opening (w), pressure (p) and fracture radius (R)

IMPROVING THE CODE NUMERICS FOR COMPLEX REAL APPLICATIONS

HI24L: complex real-world case with **32 faults** intersecting in various ways, discretized with more than **5M elements**.
It is located in the Gulf of Mexico, offshore the Texas coastline.

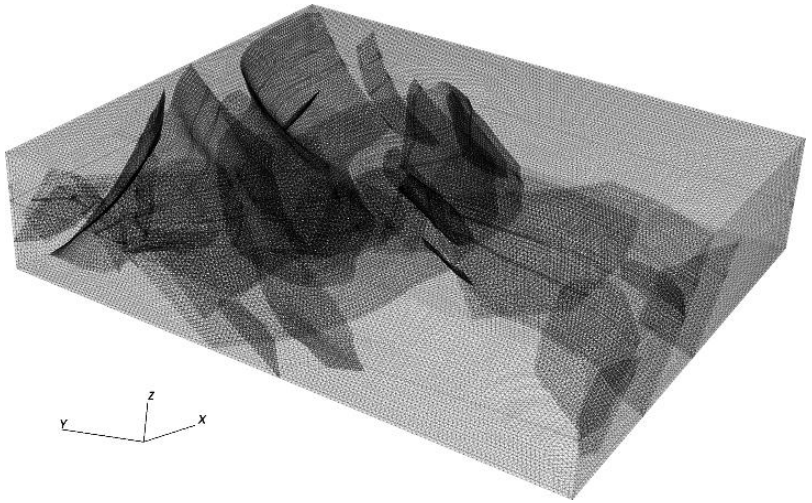

FE – IE mesh

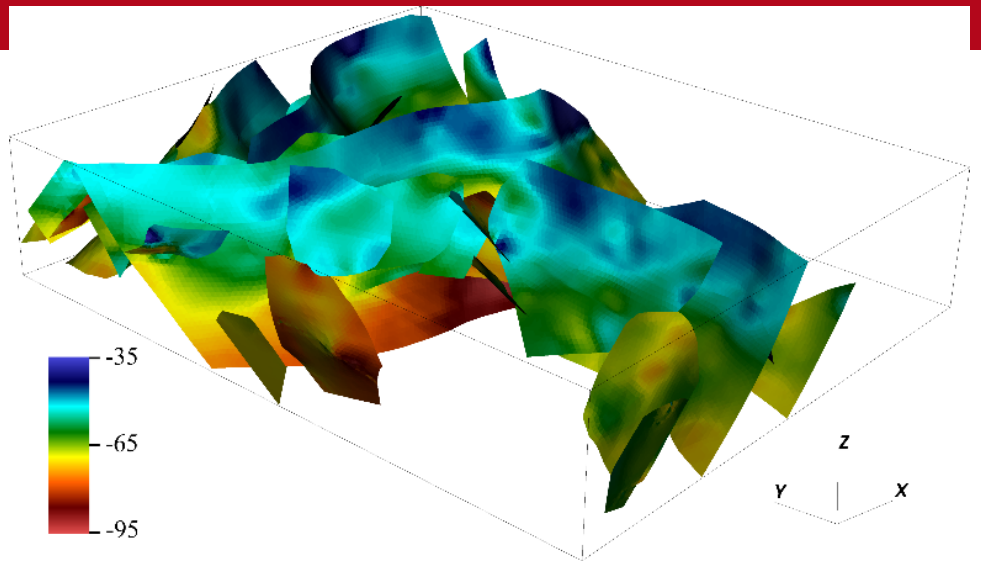

Views of the normal component of the traction field on the fracture surfaces

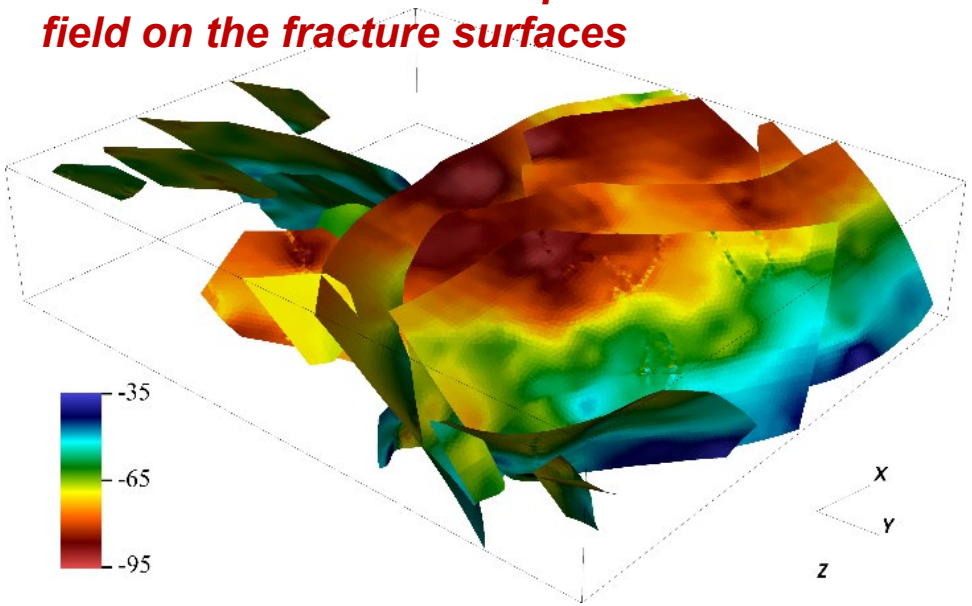

PLANNED RESEARCH

STORING GREEN ENERGY UNDERGROUND: H2 POTENTIAL IN ITALY

S1. Criteria for identification of possible geologic structures for UHS

S2. Identification and characterization of reservoirs in Italy most promising for UHS

S3. H2 fate in subsurface reservoirs

S4. Hazards related to UHS

S5. H2 – subsurface environment interactions

S6. Guidelines on incentives strategies needed to make UHS competitive

S7. UHS risk perception and social aspects

- Relationships linking the change of geomechanical properties to chemical H2-CH4-rock interactions and microbial activity will be implemented in GEPD3D to quantify the effects of these processes on the mechanical safety of UHS;

- Investigation of parameter-related model uncertainties via Sobol' indices in a generalized Polynomial Chaos Expansion (gPCE) framework. Application to outcomes of GEPS3D with quasi-static seismological relationships (Zoccarato et al, 2019);

Thank you for the attention

pietro.teatini@unipd.it

The reseasch was funded by the State Supervision of Mines, Ministry of Economic Affairs, The Netherlands